

Numerical Experiments on the Modulation Theory for the Nonlinear Atomic Chain

W. Dreyer^{a,1}, M. Herrmann^{b,2,3}

^a *Weierstrass Institute for Applied Analysis and Stochastics
Mohrenstr. 39, 10117 Berlin, Germany*

^b *Humboldt Universität zu Berlin, Institut für Mathematik,
Unter den Linden 6, 10099 Berlin, Germany*

Abstract

Modulation theory with periodic traveling waves is a powerful, but not rigorous tool to derive a thermodynamic description for atomic chains with nearest neighbor interactions (FPU chains). This theory is sufficiently complex to deal with strong oscillations on the microscopic scale, and therefore it is capable to describe the creation of temperature and the transport of heat on a macroscopic scale. In this paper we investigate the validity of modulation theory by means of several numerical experiments. We start with a survey on the foundations of modulation theory. In particular, we discuss the hyperbolic scaling, the notion of cold data, microscopic oscillations and Young measures, periodic and modulated traveling waves, and, finally, the resulting macroscopic conservation laws. Afterwards we discuss how the validity of a macroscopic theory may be tested within numerical simulations of the microscopic dynamics. To this end we describe an approach to thermodynamic data exploration which is motivated by the theory of Young measures, and relies on mesoscopic windows in space and time. The last part is devoted to several numerical experiments including examples with periodic boundary conditions and smooth initial data, and macroscopic Riemann problems. We interpret the outcome of these experiments in the framework of thermodynamics, and end up with two conclusions. 1. There are many examples for which modulation theory provides in fact the right thermodynamic description because it can predict both the structure of the microscopic oscillations and their macroscopic evolution correctly. 2. Modulation theory will fail if the oscillations exhibit a more complicate structure.

Key words: atomic chain, thermodynamic limit, periodic traveling waves, modulation theory, Riemann problems

PACS: 02.70.Ns, 05.70.Ce, 05.70.Ln, 31.15.Qg, 45.20.Dd

1 Introduction

The atomic chain with nearest neighbour interaction (FPU chain), see Figure 1, consists of N identical particles with unit mass. These are located on the real axis and are labeled by the index $\alpha = 1 \dots N$. For given α , let $x_\alpha(t)$ and

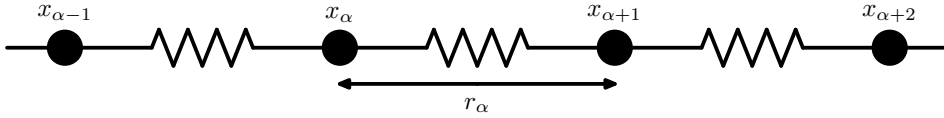


Figure 1. The atomic chain with nearest neighbour interaction.

$v_\alpha(t) = \dot{x}_\alpha(t)$ denote the position and velocity, respectively, of the atom α at time t , and let $r_\alpha(t) = x_{\alpha+1}(t) - x_\alpha(t)$ be the distance between the atoms $\alpha + 1$ and α . The dynamics of the chain is governed by Newton's law of motion

$$\ddot{x}_\alpha(t) = \Phi'(x_{\alpha+1}(t) - x_\alpha(t)) - \Phi'(x_\alpha(t) - x_{\alpha-1}(t)), \quad (1)$$

where Φ is the (nonlinear) atomic interaction potential. For our purposes it is convenient to consider distance and velocity as the independent variables. Eliminating x in (1) we find the equivalent system

$$\dot{r}_\alpha(t) = v_{\alpha+1}(t) - v_\alpha(t), \quad \dot{v}_\alpha(t) = \Phi'(r_\alpha(t)) - \Phi'(r_{\alpha-1}(t)). \quad (2)$$

Since the number of particles is finite we must impose appropriate boundary conditions, so that (2) becomes a closed system of $2N$ ODEs with unknowns $r_1 \dots r_N$ and $v_1 \dots v_N$. Here we consider only two kinds of boundary conditions. The first one describes a periodic chain, i.e. we suppose $r_0(t) = r_N(t)$ and $v_{N+1}(t) = v_1(t)$, so that the total momentum and the total energy are conserved in time. The second kind of boundary conditions allows the computation of Riemann problems and will be introduced in §3.

Newton's equations describe the evolution of the atomic chain on the *microscopic scale*, and thus we call t and α the *microscopic* time and particle index, respectively. If the number of particles N is very large, we are not interested in the complete solution to (1), but rather in its thermodynamic properties. This means, we shall describe the evolution of some averaged quantities like mean distance and mean velocity on a suitable chosen *macroscopic scale*. A micro-macro transition is a theory which can derive macroscopic evolution equations directly from (1). Unfortunately, no rigorous theory can do this without making further assumptions, but in §2 we show that one can use modulation theory

¹ E-Mail dreyer@wias-berlin.de

² E-Mail michaelherrmann@math.hu-berlin.de

³ supported by *Deutsche Forschungsgemeinschaft* (DFG) within the Priority Program SPP 1095 *Analysis, Modeling and Simulation of Multiscale Problems*

with periodic traveling waves in order to establish a micro-macro transition on a formal level.

In this paper we solely consider the macroscopic scale that results from the *hyperbolic scaling* (cf. Figure 2) as follows. We introduce the *scaling parameter* ε by $\varepsilon = 1/N$, and define the macroscopic time \bar{t} and the macroscopic particle index $\bar{\alpha}$ by

$$\bar{t} = \varepsilon t, \quad \bar{\alpha} = \varepsilon \alpha. \quad (3)$$

Note that for $N \rightarrow \infty$ the macroscopic particle index becomes a continuous

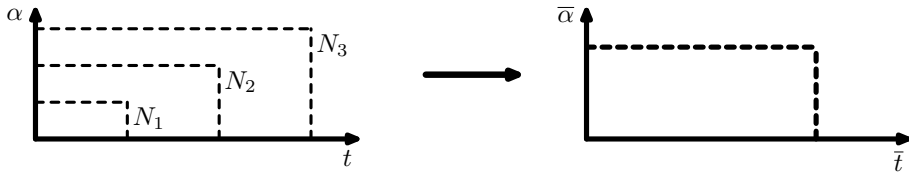


Figure 2. The hyperbolic scaling.

variable taking values in the unit interval $[0, 1]$. Moreover, we define the macroscopic space \bar{x} by $\bar{x} = \varepsilon x$, and this fixes the scaling of all other quantities. In particular, the identities $x/t = \bar{x}/\bar{t}$ and $x/\alpha = \bar{x}/\bar{\alpha}$ imply that both the distance r and the velocity v are invariant under the hyperbolic scaling. Besides (3) there are other reasonable scalings which provide macroscopic evolution equations for the atomic chain, see [DK00,SW00,GM04,GM06], and [GHM06] for an overview.

All considerations which follow are restricted to convex interaction potentials, because only in this case we can establish the micro-macro transition. A famous example is the Toda potential

$$\Phi(r) = \exp(1 - r) + r - 1, \quad (4)$$

which makes (2) completely integrable, cf. [Hén74,Fla74], but our approach to micro-macro transitions is not related to integrability, and applies to all non-linear and strict convex potentials. Moreover, our numerical results indicate that the validity of modulation theory does not depend on integrability.

Oscillatory data and thermodynamics The macroscopic description of the atomic chain becomes very complicated if the atomic data exhibit oscillations on the microscopic scale. In this case, the most challenging problem is to find an appropriate mathematical description for the macroscopic evolution of the microscopic oscillations. An elegant framework for this issue is provided by the theory of Young measures as it allows to use *probabilistic* concepts like *distributions functions* for the macroscopic description of an purely *deterministic* microscopic system. However, relying only on this theory we are

not able to establish the micro-macro transition. As we will see below, for a complete macroscopic theory we must combine the notion of Young measures with some additional assumptions concerning the structure of the microscopic oscillations. In this paper we always assume that all microscopic oscillations take the form of modulated traveling waves.

Another way to think about microscopic oscillations is in terms of thermodynamics. The key idea in this context is the following. The microscopic oscillations can be regarded as a kind of *internal motion*, in which some amount of the total energy is stored, and this observation gives rise to an intrinsic notion of *temperature*. Although strict thermodynamic concepts are not yet well established within the mathematical community, their use turn out to be very fruitful for the macroscopic description of systems with microscopic oscillations. Thermodynamics can be easily combined with the notion of Young measures, and provides an elegant language to describe macroscopic effects like the motion of mechanical waves or the transport of heat. Moreover, thermodynamical arguments allows us to extract the macroscopically relevant information from the enormous amount of data which come out from numerical simulations with large particle numbers.

Modern thermodynamics describe a macroscopic body in terms of mechanical and thermodynamical fields like pressure, temperature, and the densities for mass, momentum, and energy. In the macroscopic *Lagrangian representation* these fields depend on time \bar{t} and the material coordinate, which can be identified with the macroscopic particle index $\bar{\alpha}$. To derive a reasonable thermodynamic model for chains we follow the lines of *Rational Thermodynamics* which is based on the following two paradigms.

- 1 **First Principles.** There exist fundamental balance equations as for instance the (local) conservation laws for mass, momentum and energy. These equations are considered to be *universal*, i.e., they are supposed to hold for all materials and all processes.
- 2 **Material Laws.** The second building block are material- and process- dependent *constitutive laws* which provide pointwise relations between several thermodynamic fields. In particular, these constitutive relations guarantee that the universal balance equations become a closed system of PDEs.

Next we explain how the modulation theory with periodic traveling waves fits into this thermodynamic framework.

Notion of modulation theory In this paper we consider a special class of microscopic oscillations in FPU chains, namely those which take the form of modulated traveling waves. The thermodynamic model for their macroscopic evolution turns out to be provided by Whitham's modulation theory, and is

based on (periodic) traveling waves. A *traveling wave* is an *exact* solution to (1) which satisfies the ansatz

$$x_\alpha(t) = r\alpha + vt + \mathbb{X}(k\alpha + \omega t). \quad (5)$$

Here r , v , k , and ω are four parameters, and can be interpreted as *mean distance*, *mean velocity*, *wave number*, and *frequency*, respectively. The *wave profile* \mathbb{X} depends only on the *phase variable* $\varphi = \omega t + k\alpha$, and describes the microscopic oscillations. In what follows we solely consider periodic wave profiles with unit periodicity length, i.e., we assume $\mathbb{X}(\varphi + 1) = \mathbb{X}(\varphi)$.

A *modulated traveling wave* is not an exact but only *approximate* solution to (1) for which the traveling parameters vary on the macroscopic scale. The main issue of modulation theory is the derivation of a system of PDEs that governs the macroscopic evolution of the modulated traveling wave parameters. As we show in §2.4, this system consists of four macroscopic conservation laws

$$\partial_{\bar{t}}(r, v, k, S)(\bar{t}, \bar{\alpha}) + \partial_{\bar{\alpha}}(-v, +p, -\omega, +g)(\bar{t}, \bar{\alpha}) = 0, \quad (6)$$

which can be interpreted as the fundamental conservation laws for mass, momentum, wave number, and entropy.⁴ Moreover, the modulation equations formally imply

$$\partial_{\bar{t}}\left(\frac{1}{2}v^2 + U\right)(\bar{t}, \bar{\alpha}) + \partial_{\bar{\alpha}}(vp + \omega g)(\bar{t}, \bar{\alpha}) = 0, \quad (7)$$

which is the conservation law for the energy. The system (6) consists of four equations for seven quantities. It is closed by the *equation of state* and a *Gibbs equation*, which both are intimately related to traveling waves, see §2. The equation of state provides the internal energy U as function of mean distance r , wave number k , and entropy S , and depends on the interaction potential Φ (which embodies the material properties). All other constitutive relations are in turn determined by the universal Gibbs equation

$$dU = \omega dS - p dr - g dk. \quad (8)$$

The modulation theory described above is not completely understood for the following two reasons.

- (1) Up to now, the validity of the modulation system (6) with (8) is not justified rigorously for arbitrary potentials but only for the Toda chain, and some other very special potentials, see [Her05,DHM06]. This lack of rigor

⁴ Here, and likewise in other thermodynamic field theories as for instance the Euler system, we find a conservation law for the entropy, but we cannot not expect the entropy to be conserved across a shock solution.

was the starting point for our investigations. Our simulations provide numerical evidence that (6) and (8) describe in fact the thermodynamic limit of the atomic chain for a wide class of initial value problems.

- (2) All properties of the macroscopic system (6) are determined by the equation of state. However, this equation of state depends on the interaction potential Φ , and is almost never given explicitly. This causes several difficulties which we discuss within §2 and §3.

There exists a well established theory for modulated traveling waves in integrable systems (Toda chain, KdV equation), which relies on a careful analysis of the dynamics of systems in Lax-form, see [El05,LL83,Ven85]. Although this theory are very satisfactory from a mathematical point of view, it is very hard to carry over their concepts to non-integrable systems. More precisely, all rigorous results for the Toda chain are formulated in very special coordinates which are un-physical as they have no counterparts in non-integrable chains. For this reason we have chosen a framework built on the generic concepts of Young measures and thermodynamics, which can be applied to both integrable and non-integrable interaction potentials.

We mention that our considerations concern the modulations of *single-phase* traveling waves only. It is known for integrable system that there exists variants of modulation theory based on *two-* or even *multi-phase* traveling waves, see [BY92,DM98]. Moreover, numerical simulations in [HR07] indicate that modulated multi-phase traveling waves exists for all convex interaction potentials, but this phenomenon is not addressed in this paper.

Main issues We consider several numerical simulations of initial value problems for FPU chains with nonlinear but convex interaction potentials. We always choose the initial data from the class of modulated traveling waves, and focus on the following two objectives. Note that it is *not* our intention to present a study on accuracy, efficiency or convergence properties of numerical ODE integrators.

- (1) We study the convergence of oscillatory atomic data in the limit $N \rightarrow \infty$. The key idea is that we can expect the atomic data to converge to a unique limit in the sense of Young measures. Moreover, we describe how the thermodynamically relevant information can be extracted from the enormous amount of microscopic data. To this end we introduce *mesoscopic* space-time windows which are very small on the macroscopic scale but very large with respect to microscopic units. These windows allow us to compute *local distribution functions* of the atomic data as well as *local mean values* of microscopic observables.
- (2) We present an approach for the numerical justification of modulation theory that can be applied to all convex atomic interaction potentials.

To that purpose we show that the microscopic oscillations arising in the numerical data can in fact be described by modulated traveling waves. Finally, exploiting the theory of Young measures we can conclude that the macroscopic dynamics of the modulated parameters is governed by the modulation equations (6).

In this paper we consider two classes of initial value problems. Class S concerns finite chains with periodic boundary conditions, and here we assume that the initial modulation of the traveling wave parameters is smooth with respect to the macroscopic particle index $\bar{\alpha}$. Within the Class R we study microscopic Riemann problems for infinite chains, where in the simplest case the initial distances and velocities are piecewise constant with a single jump discontinuity.

Energy conservation as the origin of dispersive shocks Some aspects of Riemann problems have much in common with *zero dispersion limits*. To explain the basic phenomenon let us start with the famous Burgers' equation

$$\partial_{\bar{t}} u + u \partial_{\bar{\alpha}} u = 0. \quad (9)$$

which is, on a formal level, the zero dispersion limit of the KdV equation

$$\partial_{\bar{t}} u + u \partial_{\bar{\alpha}} u + \varepsilon \partial_{\bar{\alpha}}^3 u = 0. \quad (10)$$

Here, u is a scalar field depending on the macroscopic coordinates $(\bar{t}, \bar{\alpha})$, and ε is an artificial small parameter. The main question is, under which conditions the solutions to (10) converge to (weak) solutions to (9) as $\varepsilon \rightarrow 0$. The rigorous theory for this problem was developed in [LL83,Ven85] by exploiting the complete integrability of (10). It is known that for given smooth initial datum u_0 there usually exists a critical time \bar{t}_{crit} such that (9) has a unique smooth solution for $0 \leq \bar{t} < \bar{t}_{\text{crit}}$ only. At time $\bar{t} = \bar{t}_{\text{crit}}$ this solution becomes discontinuous in one point $\bar{\alpha}_{\text{crit}}$, and for $\bar{t} > \bar{t}_{\text{crit}}$ solutions exist in a weak sense only. More precisely, for $\bar{t} > \bar{t}_{\text{crit}}$ any weak solution u satisfies $\partial_{\bar{t}} u + \frac{1}{2} \partial_{\bar{\alpha}} (u^2) = 0$ in the sense of distributions. Imposing the same initial datum u_0 for KdV, the typical behavior for $\varepsilon \rightarrow 0$ is as follows, see [Lax86,Lax91,LLV93]. For $0 \leq \bar{t} < \bar{t}_{\text{crit}}$ the solutions u_ε to (10) converge in some strong sense to the unique smooth solution to (9). However, for $\bar{t} > \bar{t}_{\text{crit}}$ the KdV-solutions become highly oscillatory in a neighborhood of $\bar{\alpha}_{\text{crit}}$ with typical wavelength $1/\sqrt{\varepsilon}$. For $\bar{t} > \bar{t}_{\text{crit}}$ the functions u_ε still converge to a weak limit $\langle u \rangle$, but the main point is the following. The weak limit $\langle u \rangle$ does *not* satisfy Burgers equation, i.e. $\partial_{\bar{t}} \langle u \rangle + \frac{1}{2} \partial_{\bar{\alpha}} \langle u \rangle^2 \neq 0$, because for the weak limit $\langle u^2 \rangle$ of u_ε^2 we have $\langle u \rangle^2 \neq \langle u^2 \rangle$. Similar phenomena occur in the limit for various dispersive difference schemes, see [GL88,HL91,LL96].

We next describe the macroscopic evolution of cold data for the atomic chain

because there exists a close relation to the above mentioned phenomenon. We say the atomic data are *cold*, if there exist two macroscopic fields r and v (depending on \bar{t} and $\bar{\alpha}$) such that

$$r_\alpha(t) = r(\varepsilon t, \varepsilon \alpha), \quad v_\alpha(t) = v(\varepsilon t, \varepsilon \alpha). \quad (11)$$

Inserting this ansatz into Newton's equation (2) yields to leading order

$$\partial_{\bar{t}} r - \nabla^{+\varepsilon} v = 0, \quad \partial_{\bar{t}} v - \nabla^{-\varepsilon} \Phi'(r) = 0,$$

where $\nabla^{+\varepsilon}$, $\nabla^{-\varepsilon}$ are discrete differential operators. In the limit $\varepsilon \rightarrow 0$ we formally obtain the PDEs

$$\partial_{\bar{t}} r - \partial_{\bar{\alpha}} v = 0, \quad \partial_{\bar{t}} v - \partial_{\bar{\alpha}} \Phi'(r) = 0, \quad (12)$$

which can be viewed as the macroscopic conservation laws for mass and momentum. These equations provide a reasonable mechanical model for the evolution of a *nonlinear string*. Moreover, the same equations appear within isentropic gas dynamics, and one usually refers to these equations as the p -system (with $p = -\Phi'$). It is well known, see [Smo94,Daf00,GR96], that for convex Φ the string equations (12) form a nonlinear and strictly hyperbolic system, and imply the conservation of energy

$$\partial_{\bar{t}} \left(\frac{1}{2} v^2 + \Phi(r) \right) - \partial_{\bar{\alpha}} (v \Phi'(r)) = 0 \quad (13)$$

for all smooth solutions. Similarly to above, the string equations in fact describe the thermodynamic limit for cold atomic data as long as these data are smooth on the macroscopic scale. However, when the nonlinearity forms a shock at time \bar{t}_{crit} , the system (12) is no longer a thermodynamic consistent model for $\bar{t} > \bar{t}_{\text{crit}}$. To see this let us summarize some basic facts about shock solutions to (12). For simplicity we assume that the convex potential Φ has a strictly convex (or concave) derivative Φ' , so that all eigenvalues of (13) are genuinely nonlinear. According to the Lax theory for hyperbolic systems, see for instance [GR96,Daf00,LeF02], a shock wave propagates with a constant shock speed σ , and the basic variables r and v satisfy the Rankine-Hugoniot jump conditions across the shock. These conditions read

$$-\sigma[[r]] - [[v]] = 0, \quad -\sigma[[v]] - [[\Phi'(r)]] = 0, \quad (14)$$

where $[[\cdot]]$ denotes as usual the jump. However, (14) implies that the jump condition for the energy must be violated, i.e., for any shock with (14) we have

$$-\sigma[[\frac{1}{2}v^2 + \Phi(r)]] - [[v\Phi'(r)]] \neq 0. \quad (15)$$

Consequently, the string equations predict some production for the macroscopic energy (the Lax criterion selects the shocks with negative energy production). In contrast to (15), Newton's equations conserve mass, momentum

and energy, and for this reason the string equations cannot describe the thermodynamic limit beyond the shock. We will see in the numerical simulations that the atomic data beyond the macroscopic shock start to oscillate on the microscopic scale, and self-organize into modulated traveling waves. The arising oscillations spread out in the macroscopic space-time and give rise to a *dispersive shock wave*. This corresponds to the fact that some amount of mechanical energy is dissipated into internal energy, and shows that our notion of temperature is generic for atomic chains. It is one of the merits of modulation theory that it can describe the microscopic oscillations emerging from cold shocks.

The numerical investigation of shocks in the atomic chain started with Holian and Straub [HS78], and during the last decades a lot of research concerned Riemann problems in the Toda chain, see [HFM81,VDO91,Kam91,BY92,DM98], where the onset of dispersive shock waves is well understood. However, there is no mathematical theory for dispersive shocks in non-integrable chains, and all rigorous results for the Toda chain do not address the macroscopic behavior of the thermodynamic fields. For these reasons we return to dispersive shocks in §5.

Main results The numerical simulation presented below provide numerical evidence for the following propositions.

- (i) If all macroscopic fields are smooth, then the oscillations in the atomic data can be described in terms of modulated traveling waves, and the macroscopic dynamics is governed by the modulation system (6) with (8).
- (ii) Moreover, we can use modulated traveling waves to describe the microscopic oscillations which arise when cold data form shocks.
- (iii) If the shocks emerge from data with temperature, then usually the microscopic oscillations exhibit a more complicated structure, and modulation theory fails in this case.

In summary we can conclude that modulation theory provides the correct thermodynamic description for a wide class of problems. In particular, the theory is able to describe the creation of temperature from cold data as well as the transport of heat in a nonlinear medium. Recall that all these propositions are valid only under the following restrictions. (i) The interaction potential Φ is convex, (ii) the macroscopic scale results from the hyperbolic scaling, and (iii) the initial data are given in form of modulated traveling waves.

Outline of this paper This paper is organized as follows. In §2 we give an overview on the foundations of this study. We use the theory of Young

measures in order to derive some restrictions for the macroscopic dynamics of any reasonable thermodynamic limit under the hyperbolic scaling. Afterwards we discuss the existence and thermodynamic properties of periodic traveling waves, and give an overview on the modulation theory with periodic single-phase traveling waves as it is developed in [FV99,Her05,DHM06]. In §3 we proceed with a discussion of the numerical methods and techniques. In particular, we introduce the notion of mesoscopic space-time windows, and discuss the numerical computation of both local distribution functions and local mean values. Finally we explain how one can associate a periodic traveling waves to a given space-time window, and summarize our strategy for the numerical justification of modulation theory.

§4 contains the numerical simulations for periodic boundary conditions and initial data with smooth mean values on the macroscopic scale. We start with two examples, $S1$ and $S2$, where we impose temperature in form of microscopic oscillations already in the initial data. These two examples illustrate that the atomic data converge as $N \rightarrow \infty$ to a unique limit in the sense of Young measures. Moreover, for sufficiently small macroscopic times modulation theory turns out to be capable to describe the arising microscopic oscillations correctly. However, it may happen that the data form a macroscopic shock at a critical time \bar{t}_{crit} , and in this case modulation theory fails for $\bar{t} > \bar{t}_{\text{crit}}$. In the third example $S3$ we study the evolution of cold but smooth initial data. The atomic data remain cold for $\bar{t} < \bar{t}_{\text{crit}}$, where \bar{t}_{crit} is again the time where the first shock is formed. For $\bar{t} > \bar{t}_{\text{crit}}$ the atomic data beyond this shock self-organize into modulated traveling waves. Finally, Example $S4$ illustrates that the restriction to convex interaction potentials is essential.

The problem how macroscopic shock waves influence the validity of modulation theory is studied in more detail within §5, where we solve three macroscopic Riemann problems. In all three examples we find that in the limit $N \rightarrow \infty$ the atomic data reproduce the typical structure for solutions of Riemann problems. This means the macroscopic part of all solutions is self-similar, and consists of several waves separated by constant states. With Example $R1$ we study the contact problem for two cold half-chains, and similarly to Example $S3$ we find that microscopic oscillations arising from cold shocks take the form of modulated traveling waves. In Examples $R2$ we impose cold initial data on one half-chain but initial data with temperature on the other one. Surprisingly we find that modulation theory can predict the structure of the resulting microscopic oscillations correctly. Finally, in Example $R3$ both half-chains are initialized with temperature. The resulting microscopic oscillations exhibit a complicate structure which cannot be described by modulated traveling waves.

2 Foundations of modulation theory

2.1 Macroscopic evolution of data with temperature and Young measures

In §1, the restriction to cold data has led to the quite simple set of macroscopic equations (12). However, micro-macro transitions with oscillatory atomic data are much more involved, and call for thermodynamic concepts like temperature and heat transport. In this section we exploit the theory of Young measures, and derive some essential building blocks for the thermodynamic description of the atomic chain.

- (1) Young measures provide an elegant framework for the interpretation of our numerical experiments, and allow to identify the thermodynamic relevant properties that are independent of the particle number. Moreover, Young measures bridge between the deterministic microscopic dynamics and a probabilistic description on the macroscopic scale.
- (2) The numerical justification in §4 and §5 essentially relies on the comparison of different Young measures. More precisely, we will compare the measures produced by the numerical data with those that are predicted by modulation theory.
- (3) The theory of Young measures provide non-trivial restrictions for the macroscopic dynamics as it implies three universal macroscopic conservation laws.

In what follows we consider a rectangular domain Ω in the macroscopic Lagrangian space-time given by $\Omega = \{(\bar{t}, \bar{\alpha}) : 0 \leq \bar{t} \leq \bar{t}_{\text{fin}}, \alpha \in [0, 1]\}$, where $\bar{t}_{\text{fin}} > 0$ is a fixed macroscopic time. The main advantage of Young measures can be stated in terms of a compactness theorem.

Theorem 1 *Suppose that K is a compact subset of the two-dimensional Euclidian space, and suppose that $(Q^{(n)})_{n=1,2,\dots}$ is a sequence of functions $\Omega \rightarrow K$. Then there is a subsequence, still denoted by $Q^{(n)}$, and a family of probability measures $\Omega \ni (\bar{t}, \bar{\alpha}) \mapsto \mu(\bar{t}, \bar{\alpha}, dQ) \in \text{Prob}(K)$ such that for any continuous observable $\Psi = \Psi(Q)$ on K the following convergence is satisfied*

$$\int_{\Omega} \Psi(Q^{(n)}(\bar{t}, \bar{\alpha})) \phi(\bar{t}, \bar{\alpha}) \, d\bar{t} \, d\bar{\alpha} \xrightarrow{n \rightarrow \infty} \int_{\Omega} \langle \Psi \rangle(\bar{t}, \bar{\alpha}) \phi(\bar{t}, \bar{\alpha}) \, d\bar{t} \, d\bar{\alpha}. \quad (16)$$

Here the function $\langle \Psi \rangle$ is defined by

$$\langle \Psi \rangle(\bar{t}, \bar{\alpha}) = \int_K \Psi(Q) \mu(\bar{t}, \bar{\alpha}, dQ), \quad (17)$$

and ϕ denotes an arbitrary smooth test function.

Remarks

- (1) A proof of Theorem 1 can be found in [Tay96,Hör97,Daf00].
- (2) The subsequence provided by Theorem 1 *converges to μ in the sense of Young measures*. Usually one refers to the whole family $(\bar{t}, \bar{\alpha}) \mapsto \mu(\bar{t}, \bar{\alpha}, dQ)$ as the Young measure, whereas for a given point $(\bar{t}, \bar{\alpha}) \in \Omega$ the probability measure $\mu(\bar{t}, \bar{\alpha}, dQ)$ is called the *disintegration* of μ at this point.
- (3) According to (19) we can regard the functions $\langle \Psi \rangle$ as weak limits.
- (4) If the sequence $(Q^{(n)})_n$ converges strongly to some limit function $Q^{(\infty)}$, then (16) and (17) imply

$$\mu(\bar{t}, \bar{\alpha}, dQ) = \delta_{Q^{(\infty)}(\bar{t}, \bar{\alpha})}(dQ)$$

where $\delta_{Q_0}(dQ)$ denotes a Dirac distribution located in the point Q_0 . However, if the functions $Q^{(n)}$ are *oscillatory*, then the support of each measure $\mu(\bar{t}, \bar{\alpha}, dQ)$ will contain more than one point. In this case, the probability measure $\mu(\bar{t}, \bar{\alpha}, dQ)$ describes the *oscillations in the vicinity* of $(\bar{t}, \bar{\alpha})$, and $\langle \Psi \rangle(\bar{t}, \bar{\alpha})$ gives the *local mean value* of the observable Ψ .

- (5) Theorem 1 claims that sequences which are bounded in L^∞ are compact w.r.t. to the convergence of Young measures. There exist generalizations of this result that rely on uniform bounds in L^p with $p > 1$, but then additional assumptions on the decay behavior of the observables Ψ are needed. For simplicity we omit the details, and refer to [War99].

Next we describe how we can apply Theorem 1 in the context of micro-macro transitions for the atomic chain. For that issue we restrict to finite chains with periodic boundary conditions so that the total energy of the chain is finite and conserved during the evolution. In what follows let $(N_i)_{i=1,2,\dots}$ be a sequence of particle numbers with $N_i \rightarrow \infty$ as $i \rightarrow \infty$, and for any i let $Q_\alpha^{(i)}(t) = (r_\alpha^{(i)}(t), v_\alpha^{(i)}(t))$ be a solution to Newton's equation defined for $0 \leq t \leq N_i \bar{t}_{\text{fin}}$ and $\alpha = 1, \dots, N_i$. According to the hyperbolic scaling and the formal identification

$$Q_\alpha^{(i)}(t) \rightsquigarrow Q^{(i)}(N_i t, N_i \alpha)$$

we can regard microscopic solutions to Newton's equations as *piecewise constant* (but usually oscillatory) functions on the macroscopic domain Ω . To achieve uniform bounds we consider only those sequences $Q^{(i)}$ whose total energy is proportional to the particle number, i.e.,

$$\frac{1}{N_i} \sum_{\alpha=1}^{N_i} \left(\frac{1}{2} v_\alpha^{(i)}(0)^2 + \Phi(r_\alpha^{(i)}(0)) \right) = C + \mathcal{O}\left(\frac{1}{N_i}\right), \quad (18)$$

for some constant C independent of N_i . Such initial data usually provide solutions that are oscillatory, but (at least for macroscopic times $\bar{t}_{\text{fin}} > 0$

being not too large) bounded in L^∞ . Of course, this is rather an additional assumption, but it is satisfied in all simulations presented here. Alternatively, we could use energy conservation and (18) in order to *prove* suitable L^p -bounds for certain classes of interaction potentials, see [Her05] for the details.

Exploiting Theorem (1) we find at least a subsequence, still denoted by $(N_i)_i$, and a Young measure μ such that the identity

$$\int_{\Omega} \Psi(Q^{(i)}(N_i \bar{t}, N_i \bar{\alpha})) \phi(\bar{t}, \bar{\alpha}) \, d\bar{t} \, d\bar{\alpha} \xrightarrow{i \rightarrow \infty} \int_{\Omega} \langle \Psi \rangle(\bar{t}, \bar{\alpha}) \phi(\bar{t}, \bar{\alpha}) \, d\bar{t} \, d\bar{\alpha}. \quad (19)$$

is satisfied for all continuous observables Ψ and all smooth test functions ϕ , where $\langle \Psi \rangle$ is given by (17). In §3 we will explain how the probability measures $\mu(\bar{t}, \bar{\alpha}, dQ)$ and the mean values $\langle \Psi \rangle(\bar{t}, \bar{\alpha})$ can be computed in numerical simulations. Note that we consider the *common* probability distribution of distance and velocity instead of their separate statistics. Consequently, any measure $\mu(\bar{t}, \bar{\alpha}, dQ)$ can be interpreted as a weight function defined on the *microscopic state space* which is the plane spanned by distance and velocity.

The only assumption we made in Theorem 1 regards the existence of bounds, and therefore we cannot expect that the whole sequence $(Q^{(i)})_i$ has *only one* accumulation point in the sense of Young measures. However, in our simulations we study sequences of atomic chain for which the initial data *converge* to a modulated traveling wave. For this reason we expect to find a *unique accumulation point*, which implies convergence of the whole sequence.

In §1 we have reformulated Newton's equations as a system of first order equations with variables r and v , see (2). Since the appearing difference operators can be viewed as the discrete counterparts of the divergence operator, equations (2) can be interpreted as the *microscopic* conservation laws for mass and momentum. Moreover, (2) implies a microscopic conservation law for the atomic energy, because with $e_\alpha(t) = \frac{1}{2}v_{\alpha+1}^2(t) + \Phi(r_\alpha(t))$ and $f_\alpha(t) = -v_\alpha(t) \Phi'(r_\alpha(t))$ we find $\dot{e}_\alpha(t) = -f_\alpha(t) + f_{\alpha+1}(t)$. It is direct consequence of the microscopic conservation laws, see [Her05] for a proof, that any Young measure limit of atomic chains must satisfy the following *macroscopic* conservation laws for mass, momentum and energy.

Theorem 2 *Suppose that a sequence $(Q^{(i)})_i$ of solutions to Newton's equations converges to a Young measure μ . Then the following equations*

$$\begin{aligned} 0 &= \partial_{\bar{t}} \langle r \rangle - \partial_{\bar{\alpha}} \langle v \rangle, \\ 0 &= \partial_{\bar{t}} \langle v \rangle - \partial_{\bar{\alpha}} \langle \Phi'(r) \rangle, \\ 0 &= \partial_{\bar{t}} \langle \frac{1}{2}v^2 + \Phi(r) \rangle - \partial_{\bar{\alpha}} \langle v \Phi'(r) \rangle \end{aligned} \quad (20)$$

are satisfied.

Remarks

- (1) Apparently, the PDEs (20) constitute a restriction for any Young measure limit of the atomic chain, and can be proved by considering bounded sequences, and extracting subsequences. However, apart from these restrictions the result applies to *any kind of oscillatory data*.
- (2) In general we cannot express the fluxes in terms of the densities. The system (20) is therefore not closed, i.e., it does not determine the macroscopic evolution completely. However, the main observation is the following. If we have further information about the *pointwise structure* (pointwise in \bar{t} and $\bar{\alpha}$) of the measures $\mu(\bar{t}, \bar{\alpha}, dQ)$, then we are able to derive pointwise constitutive relations, and in this case the system (20) provides information about the *spatial and temporal evolution* of the densities. This argument plays a central role in our justification approach in §3.4.

Within modulation theory we start with some assumptions concerning the pointwise structure of the microscopic oscillations in the chain. Then we identify (i) further macroscopic evolution laws extending (20), and (ii) constitutive relations that close the extended system, so that finally we end up with a complete macroscopic model.

2.2 Existence of periodic traveling waves

In this section we summarize the most important properties of periodic traveling waves. Recall that a traveling wave is an exact solution to the atomic chain satisfying (5). Inserting this ansatz into (1) we find the advance-delay differential equation

$$\omega^2 \frac{d^2}{d\varphi^2} \mathbb{X}(\varphi) = \Phi'(r + \mathbb{X}(\varphi + k) - \mathbb{X}(\varphi)) - \Phi'(r + \mathbb{X}(\varphi) - \mathbb{X}(\varphi - k)), \quad (21)$$

where $\varphi = k\alpha + \omega t$ denotes the *phase variable*, and \mathbb{X} is the *wave profile* which describes the microscopic oscillations. For our micro-macro transition with temperature we use solely periodic traveling waves. Since the periodicity length can be chosen arbitrarily, we always suppose $\mathbb{X}(\varphi + 1) = \mathbb{X}(\varphi)$. Note that the parameter v does not appear in (21) due to the Galilean invariance of (1), but within modulation theory this additional degree of freedom becomes important.

Each periodic traveling wave provides a highly oscillatory solution to the atomic chain, and has two characteristic properties, see Figure 3.

- (1) All oscillations are caused by a constant phase shift between adjacent particles. In particular, for all α the curve $t \mapsto (r_\alpha(t), v_\alpha(t))$ has the

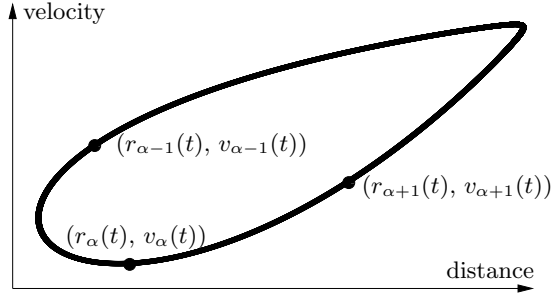


Figure 3. Schematic representation of a periodic traveling waves in the microscopic phase space. All curves $t \mapsto (r_{\alpha}(t), v_{\alpha}(t))$ differ only by a phase shift.

same image in the *microscopic phase space*, that is the plane spanned by distance and velocity. This image can be viewed as the *characteristic trace* of a traveling wave.

- (2) There is a strong coupling between oscillating distances and velocity as the trace of each periodic traveling waves is a closed curve.

At a first glance, both properties are not in accordance with our usual notion of temperature. However, any reasonable macroscopic model should describe these oscillations in the language of thermodynamics because some amount of energy is stored in these oscillations. It is the great advantage of modulation theory that it provides such a thermodynamically consistent description including temperature, internal energy, heat flux and so on.

For completeness we cite an existence result for four-parameter families of periodic traveling waves from [FV99]. A simplified proof in terms of convex analysis can be found in [DHM06]. Other existence results for periodic (or non-periodic) traveling waves are given in [FW94,AG96,FP99,FV99,PP00,Pan05].

Theorem 3 *Suppose that the convex interaction potential Φ is defined on the whole real axis, twice continuously differentiable, and satisfies $0 < m \leq \Phi'' \leq M$ for some constants m, M . Then, for each four-parameter set (r, v, k, γ) with $0 < k < 1$ and $\gamma > 0$ there exists a frequency $\omega > 0$ and a 1-periodic, smooth wave profile \mathbb{X} such that the traveling wave equation (21) as well as*

$$0 = \int_0^1 \mathbb{X}(\varphi) \, d\varphi, \quad \gamma = \frac{1}{2} \int_0^1 (\mathbb{X}'(\varphi))^2 \, d\varphi, \quad (22)$$

are satisfied.

This theorem solves the non-trivial existence problem for periodic traveling waves, but many questions remain open as the following remarks show.

Remark 4

- (1) *The restriction $0 < k < 1$ is natural as for $k = 0$ and $k = 1$ the equation (21) becomes degenerate. In some sense these limiting cases correspond*

to solitary waves, see [PP00]. Moreover, for $\gamma = 0$ there exists only the trivial solution $\mathbb{X} \equiv 0$, and there is no condition for ω in this case.

- (2) Equation (21) is invariant under shifts w.r.t. φ , so that each shifted solution provides a further solution. It is an open problem whether or not traveling waves are unique up to phase shifts.
- (3) The technical assumptions concerning the second derivative can be weakened by means of a priori estimates. In fact, it can be shown, see [Her05], that for each traveling wave with (22), and each $\gamma > 0$ we have $|X(\varphi)| \leq \sqrt{2\gamma}$. Thus we can choose m and M as function of γ , and Theorem 3 applies to all strictly convex and smooth interaction potentials, as for instance the Toda potential (4).
- (4) The approximation of the traveling waves is investigated in [DH05].
- (5) Theorem 3 provides the existence of a four-parameter family of periodic traveling waves for a wide class of nonlinear potentials, but up to now there is no result that guarantes the smooth dependence on the parameters. Nevertheless, motivated by numerical simulations we always suppose that traveling waves depend smoothly on their parameters.
- (6) For modulation theory we are interested in four-parameter families of traveling waves parametrized by (r, v, k, ω) , compare §2.4. Although not proven rigorously, numerical simulations indicate that for nonlinear potentials one can replace (at least locally) the parameter γ by ω .

For arbitrary wave number k it is hard to solve the difference-differential equation (21). However, for $k = 1/2$ equation (21) reduces to a simple Hamiltonian ODE, because (21) implies the following symmetry properties

$$R(\varphi + 1/2) = -R(\varphi), \quad V(\varphi + 1/2) = -V(\varphi), \quad (23)$$

where $R(\varphi) = \mathbb{X}(\varphi) - \mathbb{X}(\varphi - 1/2)$, and $V(\varphi) = \omega \frac{d\mathbb{X}}{d\varphi}(\varphi)$. With (23) equation (21) is equivalent to

$$\omega \frac{dR}{d\varphi}(\varphi) = 2V(\varphi), \quad \omega \frac{dV}{d\varphi}(\varphi) = \Phi'(r - R(\varphi)) - \Phi'(r + R(\varphi)). \quad (24)$$

Traveling waves with wave number $k = 1/2$ have a further remarkable property. If the atoms in the chain evolve according to such a traveling wave, any snapshot of the atomic data for fixed time will show only two distances and two velocities. In other words, depending on whether α is odd or even we have either $r_\alpha(t) = r_1(t)$ and $v_\alpha(t) = v_1(t)$, or $r_\alpha(t) = r_2(t)$ and $v_\alpha(t) = v_2(t)$. For this reason we refer to traveling waves with $k = 1/2$ as *binary oscillations*. Note that we always find $r_1(t) + r_2(t) = 2r$ and $v_1(t) + v_2(t) = 2v$, where r and v are the constant mean distance and mean velocity, respectively. Moreover, arbitrarily chosen $r_1(0)$, $r_2(0)$, and $v_1(0)$, $v_2(0)$ determine uniquely a solution to (24), and hence we can easily initialize binary oscillations in the atomic chain. This becomes useful in §4 and §5, where we choose the initial data from the class of modulated binary oscillations.

2.3 Thermodynamics for traveling waves

As mentioned in the introduction, we can regard each periodic traveling wave as a single thermodynamic state of the atomic chain. Therefore it is very natural to study the relations between the traveling wave parameters and the mean values of different atomic observables. The resulting equations are the constitutive laws of thermodynamics, depend on the *material* (i.e., on the atomistic interaction potential Φ), and provide the closure for the universal conservation laws.

In order to investigate the thermodynamic properties of traveling waves we introduce two further 1-periodic profile functions \mathbb{R} and \mathbb{V} by $\mathbb{V}(\varphi) = \frac{d}{d\varphi}\mathbb{X}(\varphi)$, and $\mathbb{R}(\varphi) = \mathbb{X}(\varphi + k/2) - \mathbb{X}(\varphi - k/2)$. These functions are related to the oscillating atomic distances and velocities in an exact traveling wave via $r_\alpha(t) = r + \mathbb{R}(k\alpha + \omega t + k/2)$, $v_\alpha(t) = v + \omega\mathbb{V}(k\alpha + \omega t)$, and the characteristic trace of the traveling waves equals the image of the curve

$$\varphi \mapsto Q^{\text{TW}}(\varphi) = (r + \mathbb{R}(\varphi + k/2), v + \omega\mathbb{V}(\varphi)). \quad (25)$$

Most of the thermodynamic quantities are defined as mean values of the oscillating atomic data in a traveling wave. We define

$$\begin{aligned} W &= \int_0^1 \Phi(r + \mathbb{R}(\varphi)) \, d\varphi && \text{internal potential energy,} \\ p &= - \int_0^1 \Phi'(r + \mathbb{R}(\varphi)) \, d\varphi && \text{pressure = negative force,} \\ K &= \frac{\omega^2}{2} \int_0^1 \mathbb{V}(\varphi)^2 \, d\varphi && \text{internal kinetic energy,} \end{aligned}$$

and $T = 2K$ *kinetic temperature*, $F = K - W$ *internal action*, $U = K + W$ *internal energy*, $E = \frac{1}{2}v^2 + U$ *total energy*, and $L = \frac{1}{2}v^2 + F$ *total action*. Note that the norm parameter γ with $\gamma = \frac{1}{2}S/\omega = \frac{1}{2} \int_0^1 \mathbb{V}(\varphi)^2 \, d\varphi$ has no physical interpretation at all, but plays an important role in the existence theorem 3.

There exist other important thermodynamic quantities which have no microscopic counterpart. It turns out that S and g , defined by

$$S := \omega \int_0^1 \mathbb{V}(\varphi)^2 \, d\varphi, \quad g := - \int_0^1 \frac{1}{2}(\mathbb{V}(\varphi + k/2) + \mathbb{V}(\varphi - k/2)) \Phi'(r + \mathbb{R}(\varphi)) \, d\varphi,$$

can be interpreted as the macroscopic *entropy density* and *entropy flux*, respectively, cf. [Her05,DHM06]. Note that all these thermodynamic quantities are constant as long as we consider exact traveling waves, but in modula-

tion theory they become fields in \bar{t} and $\bar{\alpha}$ whose evolution is described by the modulation equations (6).

As mentioned above, a fundamental question in thermodynamics concerns the constitutive relations being satisfied by the thermodynamic quantities. In [DHM06] it is proved that any (smooth) four-parameter family of traveling waves fulfils a universal *Gibbs equation*. This Gibbs equation relates all constitutive laws to a material-dependent *equation of state* which provides the parameter dependence of a single *thermodynamic potential*. Depending on the chosen set of independent variables we obtain different alternatives, which, however, are all equivalent. The main results are listed in the following table.

<i>independent variables</i>	<i>thermodynamic potential</i>	<i>Gibbs equation</i>
(r, k, γ)	$W = W(r, k, \gamma)$	$dW = \omega^2 d\gamma - p dr - g dk$
(r, k, ω)	$F = F(r, k, \omega)$	$dF = S d\omega + p dr + g dk$
(r, k, S)	$U = U(r, k, S)$	$dU = \omega dS - p dr - g dk$

The status of these identities is as follows. If the equation of state is known for a given potential Φ , then all other constitutive relations can be determined by means of the corresponding Gibbs equation. For instance, if we know how the internal energy U depends on r , k , and S , we know that pressure p and frequency ω satisfy $p(r, k, S) = -\partial_r U(r, k, S)$ and $\omega(r, k, S) = \partial_S U(r, k, S)$. However, for almost all Φ we lack explicit expressions for the equation of state, and for this reason the modulation theory for FPU chains is not completely understood. On the other hand, there are some special potentials for which explicit expressions are available. The formulas for the following two examples are derived in [Her05,DHM06].

The harmonic chain with quadratic interaction potential $\Phi(r) = c_0 + c_1 r + \frac{c_2}{2} r^2$. Here the linearity of Φ' implies that explicit expressions for all traveling waves are available. Therefore we may compute the equation of state, and obtain

$$U(r, k, S) = c_0 + c_1 r + \frac{1}{2} c_2 r^2 + \omega(k) S. \quad (26)$$

Note that the *harmonic dispersion relation* $\omega(k) = \sqrt{c_2} \sin(\pi k)/\pi$ provides the frequency ω is a function of the wave number k . However, for generic nonlinear potentials we expect that the frequency ω can be chosen as fourth independent parameter.

The hard sphere model with interaction radius r_0 . Here all atomic interactions are modeled as elastic collisions between hard spheres with radius r_0 . This gives rise to an interaction potential Φ with $\Phi(r) = +\infty$ for $r < r_0$ and $\Phi(r) = 0$ for $r \geq r_0$. Although this potential is not smooth the notion of

traveling waves may be generalized to this case, and again we are able to derive explicit expressions for traveling waves. The corresponding equation of state turns out to be

$$U(r, k, S) = \frac{1}{2} S^2 k (1 - k) / (r - r_0)^2. \quad (27)$$

We mention that the hard sphere model describes the high energy limit for certain potentials, see [Tod81] for the Toda potential, and [FM02] for Lennard-Jones potentials.

To conclude this section we discuss the connections between Young measures and traveling waves. If we consider an exact traveling waves solutions with fixed parameters on the macroscopic scale, we can regard this oscillatory solutions as a Young measure with constant disintegration. This means $\mu(\bar{t}, \bar{\alpha}, dQ) = \mu_{\text{TW}}(dQ)$ in the sense of §2.1, where the traveling wave measure $\mu_{\text{TW}}(dQ)$ is given by

$$\int_{\text{phase space}} \Psi(Q) \mu_{\text{TW}}(dQ) = \int_0^1 \Psi(Q^{\text{TW}}(\varphi)) d\varphi, \quad (28)$$

and depends on the parameters of the traveling wave. In particular, the support of $\mu_{\text{TW}}(dQ)$ equals the characteristic trace of the traveling wave, that is the image of the curve (25), and $\mu_{\text{TW}}(dQ)$ can be regarded as a *height function* on its support. Finally we mention that the averages of atomic observables with respect to $\mu_{\text{TW}}(dQ)$ coincide with our thermodynamics definitions from above. For instance, the traveling wave parameter mean distance r and mean velocity v coincide with the averaged atomic distances and velocities, respectively, and for the traveling-wave pressure p we find

$$-p = \int_0^1 \Phi'(r + \mathbb{R}(\varphi)) d\varphi = \langle \Phi' \rangle = \int_{\text{phase space}} \Phi'(r) \mu_{\text{TW}}(dQ).$$

2.4 Modulation equations

Modulation theory is a powerful tool which provides an effective dynamical model on the macroscopic scale. It was originally developed in the context of partial differential equations, see the examples in [Whi74], but can also be applied to discrete models as for instance the atomic chain, see [FP99], or the discrete nonlinear Schrödinger equation, cf. [HLM94]. The modulation theory used in this paper relies on periodic traveling waves and leads to the system of modulation equations (6). Recall that generalizations to multi-phase traveling waves are possible but this is not addressed here.

The main idea behind modulation theory is the construction of *approximate* solutions to the atomic chain (2) by allowing the traveling wave parameter to vary on the macroscopic scale. A *modulated traveling waves* is an approximate solution of Newton's equations which satisfies the following ansatz for the atomic positions

$$x_\alpha(t) = \frac{1}{\varepsilon}X(\varepsilon t, \varepsilon\alpha) + \tilde{\mathbb{X}}(\varepsilon t, \varepsilon\alpha; \frac{1}{\varepsilon}\Theta(\varepsilon t, \varepsilon\alpha)) + \mathcal{O}(\varepsilon), \quad (29)$$

where X and Θ are two macroscopic functions. The modulated traveling wave parameters now are fields in \bar{t} and $\bar{\alpha}$, and are determined as derivatives of X and Θ via

$$\begin{aligned} v(\bar{t}, \bar{\alpha}) &= \partial_{\bar{t}}X(\bar{t}, \bar{\alpha}), & r(\bar{t}, \bar{\alpha}) &= \partial_{\bar{\alpha}}X(\bar{t}, \bar{\alpha}), \\ \omega(\bar{t}, \bar{\alpha}) &= \partial_{\bar{t}}\Theta(\bar{t}, \bar{\alpha}), & k(\bar{t}, \bar{\alpha}) &= \partial_{\bar{\alpha}}\Theta(\bar{t}, \bar{\alpha}). \end{aligned} \quad (30)$$

The function $\tilde{\mathbb{X}}$ serves to model the microscopic oscillations and provides the link to traveling waves via

$$\tilde{\mathbb{X}}(\bar{t}, \bar{\alpha}; \varphi) = \mathbb{X}(r(\bar{t}, \bar{\alpha}), v(\bar{t}, \bar{\alpha}), k(\bar{t}, \bar{\alpha}), \omega(\bar{t}, \bar{\alpha}); \varphi),$$

where \mathbb{X} is a family of traveling wave profiles depending on the parameters r , v , k , and ω , as well as on the phase variable φ . To ensure that (29) yields in fact approximate solutions to (1), we cannot choose X and Θ arbitrarily, but must satisfy some restrictions. We follow Whitham's lines of thought, and use an averaged Lagrangian in order to identify the evolution equations for the macroscopic parameter modulation. We insert the ansatz (29) into the expression for the total action integral of a finite chain with periodic boundary conditions, and replace the arising sums over α by integrals with respect to the phase variable φ and the macroscopic particle index $\bar{\alpha}$. After some elementary calculations, see [FV99,DHM06] for more details, we obtain the *averaged action integral*

$$\mathcal{L}_{\text{av}}(X, \Theta) = \int_0^{\bar{t}_{\text{fin}}} \int_0^1 L(\partial_{\bar{\alpha}}X, \partial_{\bar{t}}X, \partial_{\bar{\alpha}}\Theta, \partial_{\bar{t}}\Theta) \, d\bar{\alpha} \, d\bar{t}$$

where L is the internal action of a traveling wave with parameters (r, v, k, ω) , see §2.2. According to Whitham, the modulation equations result from the *Principle of Least Action* applied to the averaged action integral. Doing so we find the Euler-Lagrange equations

$$\partial_{\bar{t}}(\partial_v L) + \partial_{\bar{\alpha}}(\partial_r L) = 0, \quad \partial_{\bar{t}}(\partial_\omega L) + \partial_{\bar{\alpha}}(\partial_k L) = 0,$$

as well as the consistency relations $\partial_{\bar{t}}r = \partial_{\bar{\alpha}}v$, and $\partial_{\bar{t}}k = \partial_{\bar{\alpha}}\omega$, which are a direct consequence of the definitions (30). This form for the modulation equations was at first derived in [FV99], and generalizes classical results of Whitham for nonlinear wave equations, see [Whi74].

In the next step we can rephrase the modulation equations in our thermodynamic language. Recall that the total action L satisfies the Gibbs equation $dL = S d\omega - p dr - g dk + v dv$, where entropy density S , pressure p , and entropy flux g are defined within §2.2. These identities reveal that the system (6) is in fact equivalent to Whitham's modulation equations. We prefer to consider the densities in (6) as the independent variables, and this gives rise to the Gibbs equations (8), where the internal energy U plays the role of the thermodynamic potential. Moreover, one can show that this system implies the conservation law (7) for the total energy $E = \frac{1}{2}v^2 + U$ with energy flux $pv + \omega g$. Note that the equation of state, which provides U as a function of the densities r , k , and S , strongly depends on the material (i.e., on the atomistic interaction potential Φ) via the corresponding family of periodic traveling waves.

As explained within §2.1, the modulation equations for r , and v , and E can be viewed as a concretization of the universal system (20) stated in Theorem 2. In fact, if we consider a sequence of solutions to Newton's equations that converge to a unique Young measure, and if we assume that in each macroscopic point $(\bar{t}, \bar{\alpha})$ the disintegration of the limit measure coincides with a periodic traveling wave, then *it follows* that the fluxes in (20) must satisfy the constitutive relations for periodic traveling waves. In this sense we can regard the system of modulation equations as an closed extension of (20).

It is an remarkable fact that Whitham's modulation theory yields a reasonable thermodynamic model consisting of universal balance equations, a universal Gibbs equation, and a material-dependent equation of state. However, up to now the modulation theory for FPU chains is not completely understood, and many questions remain open. This lack of rigorous understanding was a strong motivation for our numerical experiments. The most important open problems are the following.

- (1) In modulation theory we suppose that traveling waves depend on four independent parameters. There exist existence proofs for four-parameter families of traveling waves, see Theorem 3, but presently there are no corresponding uniqueness results.
- (2) There is no rigorous theorem which guarantees that (i) the equation of state is unique, and (ii) the modulation equations are hyperbolic or even strictly hyperbolic.
- (3) For almost all potentials the equation of state is not known explicitly, and therefore we cannot solve the system (6) in these cases.
- (4) There is no rigorous justification, except for some special atomistic interaction potentials. We refer to [DHM06], which contains a conjecture for the general case as well as rigorous proof of this conjecture for the harmonic chain and the hard sphere model. Moreover, [Mie06] gives another rigorous justification for the harmonic chain in terms of discrete Wigner

measures.

In the next section we describe how we can test the validity of modulation theory without solving the PDE system (6). Here we proceed with some special cases for which the corresponding modulation system is completely understood. The first example is the harmonic chain. According to (6) and (26), the modulation equations read

$$\partial_{\vec{t}}(r, v, k, S)(\vec{t}, \vec{\alpha}) - \partial_{\vec{\alpha}}(v, r, \omega(k), \omega'(k)S)(\vec{t}, \vec{\alpha}) = 0. \quad (31)$$

Note that (31) splits into two independent 2×2 -systems. The first one has variables r and v , and is equivalent to the linear wave equation. The second independent subsystem governs the evolution of wave number k and entropy S , where the equation for k is even independent of S . We mention that both subsystems have their own energy balance whose sum gives (7). The second example with explicit equation of state is the hard sphere model, cf. (27). For shortness we omit explicit formulas and refer to [DHM06] for the details. The third special case concerns cold data whose macroscopic evolution is governed by the nonlinear string equations (12), see §1. Cold data have no microscopic oscillations, and this implies that (i) temperature T , entropy S and heat flux q must vanish, and (ii) wave number k and frequency ω have no meaning at all. Nevertheless, the conservation laws for mass, momentum and energy follow from (6) by setting $U = \Phi(r)$.

3 Numerical methods and techniques

3.1 Numerical integrator, initial data and time steps

The numerical integration of (1) relies on Verlet's method, a symplectic integrator of second order, see [HLW02, SYS97]. The one-step formulation of the scheme reads

$$\begin{aligned} x_{\alpha}^{(i+1)} &= x_{\alpha}^{(i)} + h v_{\alpha}^{(i)} + \frac{h^2}{2} p_{\alpha}^{(i)}, \\ v_{\alpha}^{(i+1)} &= v_{\alpha}^{(i)} + \frac{h}{2} (p_{\alpha}^{(i+1)} + p_{\alpha}^{(i)}), \\ p_{\alpha}^{(i)} &= \Phi'(x_{\alpha+1}^{(i)} - x_{\alpha}^{(i)}) - \Phi'(x_{\alpha}^{(i)} - x_{\alpha-1}^{(i)}). \end{aligned} \quad (32)$$

Here $h = \Delta t$ is the microscopic time step, and the upper index (i) denotes the i th time step. Recall that for given N the particle index α takes values in $\{1 \dots N\}$.

We cannot expect modulation theory to be valid for all classes of atomic initial

data, but must choose the initial data from the class of modulated traveling waves. For the sake of simplicity we solely consider initial data taking the form of modulated *binary oscillations*, these are modulated traveling waves with constant wave number $k = 1/2$, because in this case the explicit knowledge of the profile functions is not necessary, see §2. In fact, in order to initialize the atomic chain with modulated binary oscillations we choose four macroscopic functions r^{odd} , r^{even} and v^{odd} , v^{even} , and set

$$r_\alpha(0) = \begin{cases} r^{\text{odd}}(\varepsilon\alpha) & \text{if } \alpha \text{ is odd,} \\ r^{\text{even}}(\varepsilon\alpha) & \text{if } \alpha \text{ is even,} \end{cases} \quad v_\alpha(0) = \begin{cases} v^{\text{odd}}(\varepsilon\alpha) & \text{if } \alpha \text{ is odd,} \\ v^{\text{even}}(\varepsilon\alpha) & \text{if } \alpha \text{ is even.} \end{cases} \quad (33)$$

These initial conditions (33) are cold, if and only if $r^{\text{odd}} = r^{\text{even}}$ and $v^{\text{odd}} = v^{\text{even}}$. For periodic chains the functions r^{odd} , r^{even} , v^{odd} and v^{even} are assumed to be 1-periodic, whereas for Riemann problems they are piecewise constant with a single jump discontinuity within the interval $(0, 1)$. We mention, that the class of modulated binary oscillation is not stable during the evolution. In other words, even if we start with unmodulated wave numbers at $\bar{t} = 0$, we find non-constant wave numbers for $\bar{t} > 0$.

For initial value problems of Class S we use the boundary conditions $x_0^{(i)} = x_N^{(i)} - L$ and $x_{N+1}^{(i)} = x_1^{(i)} + L$, where the *total length* L is fixed by the initial data. These conditions describe periodic chains as they imply $r_0^{(i)} = r_N^{(i)}$ and $v_{N+1}^{(i)} = v_1^{(i)}$. For the numerical solution of Riemann problems (Class R) we set $x_0^{(i)} = x_1^{(i)} + x_2^{(i)} - x_3^{(i)}$ and $x_{N+1}^{(i)} = x_N^{(i)} + x_{N-1}^{(i)} - x_{N-2}^{(i)}$, and this gives $r_0^{(i)} = r_2^{(i)}$ and $v_{N+1}^{(i)} = r_{N-1}^{(i)}$. This kind of boundary conditions are appropriate, because we restrict the initial data to modulated binary oscillations, but they can produce reasonable results only for sufficiently small times. In fact, when the first macroscopic wave hits the boundary of the computational domain, we must stop the numerical computations.

In all simulations we solve Newton's equations (1) by means of (32) within a given macroscopic time interval $[0, \bar{t}_{\text{fin}}]$, and use always a constant time step Δt . In particular, the number of time steps is proportional to the particle number. We choose Δt small in comparison to the smallest inverse frequency t_{lin} of the linearized problem. The value of t_{lin} can be approximated by the period t_{BO} of the linearized binary oscillator, i.e. $t_{\text{lin}} \approx t_{\text{BO}}$ with $t_{\text{BO}}^{-2} = \Phi''(\bar{r})/4\pi^2$. Here \bar{r} denotes the local mean value of the atomic distances, and can be estimated during the computation. Although modulated binary oscillations create modulated traveling waves with $k \neq 1/2$, we can expect (at least for moderate macroscopic times) the resulting periodicity times t_{TW} to remain comparable with t_{BO} , i.e., $t_{\text{lin}} \approx t_{\text{TW}} \approx t_{\text{BO}}$. In all simulation we have ensured that $\Delta t/t_{\text{BO}} \lesssim 0.01$ holds during the whole computation.

<code>N</code>	: number of particles N ,
<code>ma_final_time</code>	: macroscopic final time \bar{t}_{fin} ,
<code>mi_final_time</code>	: microscopic final time $t_{\text{fin}} = N\bar{t}_{\text{fin}}$,
<code>mi_time_delta</code>	: length of microscopic time steps Δt ,
<code>mi_time_steps</code>	: number of microscopic time steps,
<code>mv_win_t_len</code>	: parameter $A_{\text{T}}^{\mathcal{F}}$ for MV-windows,
<code>mv_win_p_len</code>	: value of $2A_{\text{P}}^{\mathcal{F}} + 1$ for MV-windows,
<code>df_win_t_len</code>	: parameter $A_{\text{T}}^{\mathcal{F}}$ for DF-windows,
<code>df_win_p_len</code>	: value of $2A_{\text{P}}^{\mathcal{F}} + 1$ for DF-windows,
<code>df_win_prm</code>	: parameter $M_{\text{r}}^{\mathcal{F}} = M_{\text{v}}^{\mathcal{F}}$ for DF-windows.

Table 1

Meaning of the numerical parameters. \diamond

3.2 Windows in space and time

In order to study the macroscopic behavior of the atomic chain for large N we shall pass from the enormous amount of microscopic data to the characteristic macroscopic quantities. These are (i) the macroscopic fields of the local mean values, and (ii) the local distribution functions of the atomic data. The main tool for computing these quantities are *mesoscopic space-time windows*. These windows are very small on the macroscopic scale but contain many particles as well as many time steps. In the sequel let $\mathcal{F} = I_{\text{T}}^{\mathcal{F}} \times I_{\text{P}}^{\mathcal{F}}$ be such a window, where $I_{\text{T}}^{\mathcal{F}}$ and $I_{\text{P}}^{\mathcal{F}}$ denote sets of time steps and particle indices, respectively. This reads

$$I_{\text{T}}^{\mathcal{F}} = \left\{ i^{\mathcal{F}} - A_{\text{T}}^{\mathcal{F}} + 1, \dots, i^{\mathcal{F}} \right\}, \quad I_{\text{P}}^{\mathcal{F}} = \left\{ \alpha^{\mathcal{F}} - A_{\text{P}}^{\mathcal{F}}, \dots, \alpha^{\mathcal{F}}, \dots, \alpha^{\mathcal{F}} + A_{\text{P}}^{\mathcal{F}} \right\},$$

where $i^{\mathcal{F}}$ is a time step, $\alpha^{\mathcal{F}}$ is a particle index, and $A_{\text{P}}^{\mathcal{F}}, A_{\text{T}}^{\mathcal{F}}$ are two integers satisfying $1 \ll A_{\text{P}}^{\mathcal{F}}, A_{\text{T}}^{\mathcal{F}} \ll N$. If $t^{\mathcal{F}}$ denotes the microscopic time corresponding to $i^{\mathcal{F}}$, the window \mathcal{F} contains all microscopic data around its *macroscopic center* $Z^{\mathcal{F}} = (\varepsilon t^{\mathcal{F}}, \varepsilon \alpha^{\mathcal{F}})$.

For any atomic observable ψ we can compute its mean value $\langle \psi \rangle_{\mathcal{F}}$ with respect to \mathcal{F} . If ψ is a one-particle observable we immediately find

$$\langle \psi \rangle_{\mathcal{F}} = \frac{1}{A_{\text{T}}^{\mathcal{F}}(2A_{\text{P}}^{\mathcal{F}} + 1)} \sum_{(i, \alpha) \in \mathcal{F}} \psi(r_{\alpha}^{(i)}, v_{\alpha}^{(i)}), \quad (34)$$

and if ψ depends on more than one particle index similar formulae for $\langle \psi \rangle_{\mathcal{F}}$ can be easily derived. We mention that (34) can be regarded as the discrete analogue of (17), i.e. if the atomic data converge as $N \rightarrow \infty$ in the sense of Young measures, then $\langle \psi \rangle_{\mathcal{F}}$ is a good approximation of $\langle \psi \rangle(\varepsilon t^{\mathcal{F}}, \varepsilon \alpha^{\mathcal{F}})$.

Next we describe how we compute the distribution functions of the atomic data within a given window \mathcal{F} . As mentioned before, we always consider the

distribution functions in the microscopic phase space, that is the plane spanned by atomic distance and atomic velocity. For any \mathcal{F} we choose a rectangle $B^{\mathcal{F}}$ with

$$B^{\mathcal{F}} = \left\{ (r, v) : r_{\min}^{\mathcal{F}} < r \leq r_{\max}^{\mathcal{F}}, \quad v_{\min}^{\mathcal{F}} < v \leq v_{\max}^{\mathcal{F}} \right\},$$

and decompose it into $M_r^{\mathcal{F}} \times M_v^{\mathcal{F}}$ equal and pairwise disjoint sub-rectangles

$$B^{\mathcal{F}} = \bigcup_{m_r=1..M_r^{\mathcal{F}}, m_v=1..M_v^{\mathcal{F}}} B_{m_r, m_v}^{\mathcal{F}},$$

where $M_r^{\mathcal{F}}$ and $M_v^{\mathcal{F}}$ are two integers controlling the resolution. We approximate the atomic distribution function within \mathcal{F} by a $M_r^{\mathcal{F}} \times M_v^{\mathcal{F}}$ -matrix $W^{\mathcal{F}}$ with components

$$W_{m_r, m_v}^{\mathcal{F}} = \mu^{\mathcal{F}} \# \left\{ (i, \alpha) \in \mathcal{F} : (r_{\alpha}^{(i)}, v_{\alpha}^{(i)}) \in B_{m_r, m_v}^{\mathcal{F}} \right\}.$$

Here $\#$ means the number of elements, and $\mu^{\mathcal{F}}$ is a normalization constant. It is obvious that the matrix $W^{\mathcal{F}}$ approximates the distribution function of the atomic data only if the rectangle $B^{\mathcal{F}}$ is sufficiently large. In particular, for all $(i, \alpha) \in \mathcal{F}$ the point $(r_{\alpha}^{(i)}, v_{\alpha}^{(i)})$ must be an element of $B^{\mathcal{F}}$. For this reason we determine the bounds of $B^{\mathcal{F}}$ not a-priori but during the numerical simulation. The computation of the microscopic distribution functions is closely related to the notion of Young measures. More precisely, if the atomic data converge as $N \rightarrow \infty$ in the sense of Young measures, then the matrix $W^{\mathcal{F}}$ encodes all information about the probability measure $\mu(\varepsilon t^{\mathcal{F}}, \varepsilon \alpha^{\mathcal{F}}, dQ)$ from Theorem 1.

As mentioned above, each window \mathcal{F} is supposed to be mesoscopic. This leads to the ansatz

$$A_{\Gamma}^{\mathcal{F}} = c N^{\kappa}, \quad (2A_{\Gamma}^{\mathcal{F}} + 1) = c N^{\kappa},$$

where c is an arbitrary chosen constant, and κ is some exponent with $0 < \kappa < 1$. If the assumptions of modulation theory are satisfied, then as $N \rightarrow \infty$ all resulting local distribution functions and mean values must be independent of the particular choice of c and κ . However, for any finite N the concrete values of c and κ apparently affect the quality of the results. Moreover, if the windows are too small, then the mean values will do not vary on the macroscopic, but on some intermediate scale. On the other hand, for the evaluation of the distribution functions the windows should be rather small so that the fine structure of the microscopic oscillations become as clear as possible. For this reasons we distinguish between *MV-windows* and *DF-windows* for the computation of mean values and distribution functions, respectively, and chose the size of the windows for each simulation separately.

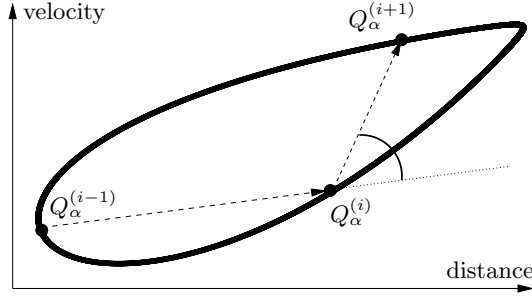


Figure 4. On the computation of the frequency ω . The auxiliary variable Ψ_ω is the rescaled angle between $Q_\alpha^{(i+1)} - Q_\alpha^{(i)}$ and $Q_\alpha^{(i)} - Q_\alpha^{(i-1)}$. \diamond

3.3 The traveling wave within a window

If the atomic oscillations are equivalent to those from modulated traveling waves, then the microscopic distributions functions within any space-time window \mathcal{F} must be equivalent to the distribution function of an exact traveling wave (whose parameters depend on \mathcal{F}). As discussed in §2, for each window \mathcal{F} we have to identify four traveling wave parameters, namely the specific length $r_{\mathcal{F}}$, the mean velocity $v_{\mathcal{F}}$, the wave number $k_{\mathcal{F}}$, and a fourth parameter which might be either the frequency $\omega_{\mathcal{F}}$, the parameter $\gamma_{\mathcal{F}}$, the entropy $S_{\mathcal{F}}$, or the temperature $T_{\mathcal{F}}$.

The values of mean distance and of mean velocity are fixed by their physical meaning, i.e., $r_{\mathcal{F}}$ and $v_{\mathcal{F}}$ result as the local mean values of the atomic distances and velocities, respectively. This means $r_{\mathcal{F}} := \langle r \rangle_{\mathcal{F}}$ and $v_{\mathcal{F}} := \langle v \rangle_{\mathcal{F}}$. Similarly, the temperature $T_{\mathcal{F}}$ is computed as twice the mean internal kinetic energy, and reads $T_{\mathcal{F}} := \langle (v - \langle v \rangle_{\mathcal{F}})^2 \rangle_{\mathcal{F}} = \langle v^2 \rangle_{\mathcal{F}} - \langle v \rangle_{\mathcal{F}}^2$. The determination of the wave number $k_{\mathcal{F}}$ and the frequency $\omega_{\mathcal{F}}$ is not so obvious as they have no immediate physical interpretation on the microscopic scale. For this reason we introduce *auxiliary observables* Ψ_k and Ψ_ω , cf. Figure 4, and set

$$k_{\mathcal{F}} := \langle \Psi_k \rangle_{\mathcal{F}}, \quad \omega_{\mathcal{F}} := \langle \Psi_\omega \rangle_{\mathcal{F}}. \quad (35)$$

The auxiliary variables in our simulations are given by

$$(\Psi_k)_\alpha^{(i)} := \frac{\text{ang}(P_{\alpha-1}^{(i)}, P_\alpha^{(i)})}{2\pi}, \quad (\Psi_\omega)_\alpha^{(i)} := \left| \frac{\text{ang}(P_\alpha^{(i-1)}, P_\alpha^{(i)})}{2\pi \Delta t} \right|, \quad (36)$$

where $P_\alpha^{(i)} = Q_{\alpha+1}^{(i)} - Q_\alpha^{(i)}$, $Q_\alpha^{(i)} = (r_\alpha^{(i)}, v_\alpha^{(i)})$, and $\text{ang}(P_1, P_2)$ denotes the angle between $P_1 = (r_1, v_1)$ and $P_2 = (r_2, v_2)$, i.e.,

$$\text{ang}(P_1, P_2) = \text{sgn}(+r_1 v_2 - r_2 v_1) \arccos \left(\frac{r_1 r_2 + v_1 v_2}{|P_1| |P_2|} \right).$$

By construction, Ψ_k takes values in $[0, 1]$, and Ψ_ω is non-negative. The formu-

lae (35)–(36) have been tested with exact traveling wave solutions, for which they reproduce the right values for $k_{\mathcal{F}}$ and $\omega_{\mathcal{F}}$. Finally, we define the entropy density $S_{\mathcal{F}}$ consistent to §2 by $S_{\mathcal{F}} := T_{\mathcal{F}}/\omega_{\mathcal{F}}$.

Atomic observable	Definition
distance	$r_{\alpha}(t) = x_{\alpha+1}(t) - x_{\alpha}(t)$
velocity	$v_{\alpha}(t) = \dot{x}_{\alpha}(t)$
negative force	$p_{\alpha}(t) = -\Phi'(r_{\alpha}(t))$
energy	$e_{\alpha}(t) = \frac{1}{2}(v_{\alpha+1}(t))^2 + \Phi(r_{\alpha}(t))$
energy flux	$f_{\alpha}(t) = -v_{\alpha}(t) \Phi'(r_{\alpha}(t))$

Table 2
Selected atomic observables.◊

In the next step we exploit the values $r_{\mathcal{F}}$, $v_{\mathcal{F}}$, $k_{\mathcal{F}}$ and $T_{\mathcal{F}}$ in order to associate an exact traveling wave to any window \mathcal{F} . For this purpose we use an approximation scheme for traveling waves described in [DH05]. To be more precise, we use the T -scheme which allows to prescribe the temperature. This scheme provides two profile functions $\mathbb{R}_{\mathcal{F}}$ and $\mathbb{V}_{\mathcal{F}}$, that describe the oscillating atomic distances and velocities in the exact traveling wave. Moreover, the scheme yields a frequency $\omega_{\mathcal{F}}^{\text{TW}}$ which does not result from the auxiliary observable Ψ_{ω} , but satisfies a dispersion relation. Employing $\omega_{\mathcal{F}}^{\text{TW}}$ and the profile functions $\mathbb{R}_{\mathcal{F}}$ and $\mathbb{V}_{\mathcal{F}}$ we can (i) derive the corresponding distribution function, (ii) define an entropy $S_{\mathcal{F}}^{\text{TW}}$ by $S_{\mathcal{F}}^{\text{TW}} = T_{\mathcal{F}}^{\text{TW}}/\omega_{\mathcal{F}}^{\text{TW}}$, and (iii) compute a *TW-mean value* $\langle \psi \rangle_{\mathcal{F}}^{\text{TW}}$ for any observable ψ . For instance, according to §2.3 the TW-pressure $p_{\mathcal{F}}^{\text{TW}}$ is given by $p_{\mathcal{F}}^{\text{TW}} = -\int_0^1 \Phi'(r_{\mathcal{F}} + \mathbb{R}_{\mathcal{F}}(\varphi + k_{\mathcal{F}}/2)) \, d\varphi$.

Note that there is a fundamental difference between mean values and *TW*-mean values. A mean value $\langle \psi \rangle_{\mathcal{F}}$ is computed directly from the numerical data, i.e., it is derived from the (approximate) *solution* of Newton's equations. On the contrary, a *TW*-mean value $\langle \psi \rangle_{\mathcal{F}}^{\text{TW}}$ is computed by means of the *TW*-profiles $\mathbb{R}_{\mathcal{F}}$ and $\mathbb{V}_{\mathcal{F}}$, and thus it reflects our *assumptions* on the microscopic oscillations. Since the profile functions $\mathbb{R}_{\mathcal{F}}$ and $\mathbb{V}_{\mathcal{F}}$ are determined by means of $r_{\mathcal{F}}$, $v_{\mathcal{F}}$, $k_{\mathcal{F}}$, and $T_{\mathcal{F}}$, the identities $r_{\mathcal{F}}^{\text{TW}} = r_{\mathcal{F}}$, $v_{\mathcal{F}}^{\text{TW}} = v_{\mathcal{F}}$, $k_{\mathcal{F}}^{\text{TW}} = k_{\mathcal{F}}$, and $T_{\mathcal{F}}^{\text{TW}} = T_{\mathcal{F}}$ are satisfied by construction. However, it is not ensured by our definitions that $\omega_{\mathcal{F}} = \omega_{\mathcal{F}}^{\text{TW}}$, $S_{\mathcal{F}} = S_{\mathcal{F}}^{\text{TW}}$, or $\langle \psi \rangle_{\mathcal{F}} = \langle \psi \rangle_{\mathcal{F}}^{\text{TW}}$ for all observables ψ . The validity of these identities must be checked!

In Table 2 we have summarized the most important atomic observables. The corresponding mean values and further derived quantities are described in Table 3. From now on we refer to the distribution functions resulting directly from the atomic data as the *microscopic distribution functions*. On the other hand, since the traveling wave parameters $r_{\mathcal{F}}$, $v_{\mathcal{F}}$, $k_{\mathcal{F}}$, and $T_{\mathcal{F}}$ vary on the macroscopic scale, we call the distribution functions determined by $\mathbb{R}_{\mathcal{F}}$ and $\mathbb{V}_{\mathcal{F}}$ the *macroscopic predictions*. Moreover, to distinguish between the different notions of mean values, we refer to $\langle \psi \rangle_{\mathcal{F}}$ and $\langle \psi \rangle_{\mathcal{F}}^{\text{TW}}$ as *fields* and *TW-fields*,

	mean value	TW-mean value
mean distance	$r_{\mathcal{F}} = \langle \text{distance} \rangle_{\mathcal{F}}$	$r_{\mathcal{F}}^{\text{TW}} = \langle \text{distance} \rangle_{\mathcal{F}}^{\text{TW}}$
mean velocity	$v_{\mathcal{F}} = \langle \text{velocity} \rangle_{\mathcal{F}}$	$v_{\mathcal{F}}^{\text{TW}} = \langle \text{velocity} \rangle_{\mathcal{F}}^{\text{TW}}$
pressure macroscopic	$p_{\mathcal{F}} = \langle \text{neg. force} \rangle_{\mathcal{F}}$	$p_{\mathcal{F}}^{\text{TW}} = \langle \text{neg. force} \rangle_{\mathcal{F}}^{\text{TW}}$
energy density macroscopic	$e_{\mathcal{F}} = \langle \text{energy} \rangle_{\mathcal{F}}$	$e_{\mathcal{F}}^{\text{TW}} = \langle \text{energy} \rangle_{\mathcal{F}}^{\text{TW}}$
energy flux	$f_{\mathcal{F}} = \langle \text{energy flux} \rangle_{\mathcal{F}}$	$f_{\mathcal{F}}^{\text{TW}} = \langle \text{energy flux} \rangle_{\mathcal{F}}^{\text{TW}}$
	field	TW-field
frequency	$\omega_{\mathcal{F}}$ is mean value	$\omega_{\mathcal{F}}^{\text{TW}}$ from T -Scheme
entropy	$S_{\mathcal{F}} = T_{\mathcal{F}}/\omega_{\mathcal{F}}$	$S_{\mathcal{F}}^{\text{TW}} = T_{\mathcal{F}}^{\text{TW}}/\omega_{\mathcal{F}}^{\text{TW}}$
heat flux	$q_{\mathcal{F}} = f_{\mathcal{F}} - p_{\mathcal{F}} v_{\mathcal{F}}$	$q_{\mathcal{F}}^{\text{TW}} = f_{\mathcal{F}}^{\text{TW}} - p_{\mathcal{F}}^{\text{TW}} v_{\mathcal{F}}^{\text{TW}}$
entropy flux	$g_{\mathcal{F}} = q_{\mathcal{F}}/\omega_{\mathcal{F}}$	$g_{\mathcal{F}}^{\text{TW}} = q_{\mathcal{F}}^{\text{TW}}/\omega_{\mathcal{F}}^{\text{TW}}$

Table 3

Mean values and derived fields. \diamond

respectively.

3.4 Strategy for the numerical justification

At a first glance the numerical justification of modulation theory should split into the following two steps. At first we solve the macroscopic modulation equations (6) by means of an appropriate PDE solver. Afterwards we compare the solutions of (6) with the corresponding macroscopic mean values derived from the numerical solution of Newton's equation. However, this direct approach is impracticable for the following reason. The main problem is that we do not know the closure relations in (6) explicitly but only in terms of traveling waves. As a consequence, any call of the flux function within the PDE solver requires a numerical integration of the difference-differential equation (21) as well as the numerical computation of some TW-mean values. Since this leads to a tremendously high numerical effort, we cannot solve the system (6) numerically, and thus the direct approach is impracticable.

Our strategy to investigate the validity of modulations theory is different from the direct approach sketched above, and has the advantage that the traveling wave equation (21) must be solved a few times only. We mainly rely on a direct comparison between the microscopic oscillations and the macroscopic predictions coming from modulation theory, where this comparison is carried out in several space-time windows. To obtain further evidence we will additionally compare some macroscopic fields with their corresponding TW-fields.

Whenever the macroscopic predictions equal the microscopic distribution functions in a given window \mathcal{F} , we can conclude that the oscillations within \mathcal{F} can

indeed by described by a traveling wave with parameters $r_{\mathcal{F}}$, $v_{\mathcal{F}}$, $k_{\mathcal{F}}$ and $T_{\mathcal{F}}$. Moreover, if we obtain such an agreement for every selected window, we have evidence that all microscopic oscillations are produced by a modulated traveling wave, and this is apparently a strong indication that modulation theory provides the correct thermodynamic description of the atomic chain.

Note that we do *not* compute the macroscopic derivatives of the macroscopic mean values, because the accurate computation of derivatives requires much larger particle numbers than the computation of the mean values. As a consequence, we do not check explicitly whether or not the modulated parameters evolve according to (6). Nevertheless, the theory of Young measures provides some a posteriori information about the macroscopic dynamics of the modulated traveling wave parameters. This will be explained now.

According to §2.1 we know that as $N \rightarrow \infty$ the local mean values of the atomic data satisfy the conservation laws of mass, momentum and energy, see (20) in Theorem 2. Recall that this property can be proved without any assumption on the structure of the microscopic oscillations. Now let us suppose that all atomic oscillations are equivalent to the oscillations in a modulated traveling wave, and consider a mesoscopic window \mathcal{F} around an arbitrary macroscopic center $(\bar{t}, \bar{\alpha})$. Due to our assumption we can express the measure $\mu(\bar{t}, \bar{\alpha}, dQ)$ in terms of a corresponding exact traveling wave, see (28). In particular, for any one-particle observable ψ we find that its mean value $\langle \psi \rangle_{\mathcal{F}}(\bar{t}, \bar{\alpha})$ must equal the corresponding TW-mean value $\langle \psi \rangle_{\mathcal{F}}^{\text{TW}}(\bar{t}, \bar{\alpha})$. Since according to Table 2 all densities and fluxes in (20) are defined as mean values of one-particle observables, the system (20) is just a subsystem of the modulation system (6)–(7). Consequently, our assumption concerning the (point-wise) structure of the microscopic oscillations implies that at least three independent modulation equations are satisfied. Of course, this does not guarantee the forth independent evolution equation (conservation of wave number) to be satisfied, but provides strong indication that modulation theory describes the macroscopic dynamics correctly.

4 Simulations with smooth initial data

All results of the numerical simulations are presented graphically. For fixed macroscopic time \bar{t} we plot the atomic data and macroscopic fields as snapshots against the macroscopic particle index $\bar{\alpha} \in [0, 1]$, and all microscopic distribution functions are presented as density plots.

Example S1

We study the evolution of initial data with temperature, i.e. with microscopic oscillations. To this end we consider a periodic Toda chain, and set

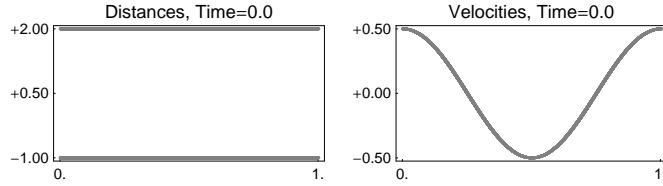


Figure 5. Example *S1*. Initial data with temperature, plotted against $\bar{\alpha}$. \diamond

$$v^{\text{odd}}(\bar{\alpha}) = v^{\text{even}}(\bar{\alpha}) = \frac{1}{2} \cos(2\pi\varepsilon\alpha), \quad r_{\text{even}}(\bar{\alpha}) = 2, \quad r_{\text{even}}(\bar{\alpha}) = -1, \quad (37)$$

cf. Figure 5. The initial atomic distances oscillate on the microscopic scale, and we mention that the velocities become likewise oscillating for $\bar{t} > 0$. Note that at $\bar{t} = 0$ we modulate only the macroscopic velocity v but neither the specific length r , the wave number k nor the temperature T .

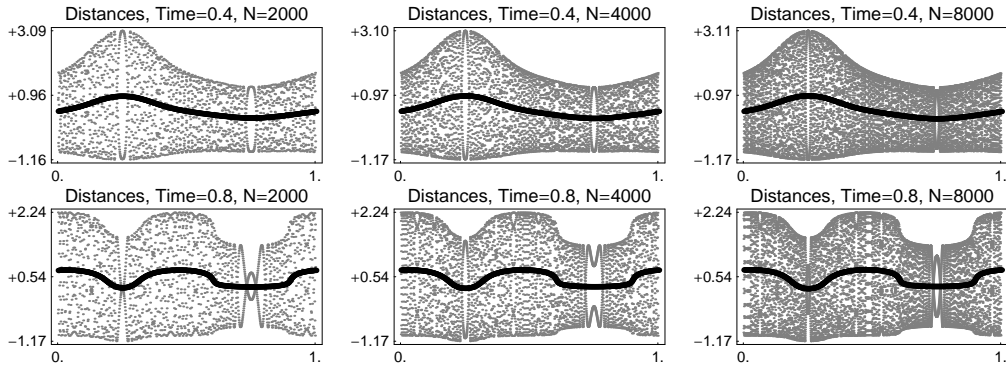


Figure 6. Example *S1*. Atomic distances plotted against $\bar{\alpha}$. The different columns correspond to the particle numbers $N = 2000$, $N = 4000$, and $N = 8000$, top and bottom row to $\bar{t} = 0.4$ and $\bar{t} = 0.8$, respectively. The dark colored functions represent the macroscopic mean values. \diamond

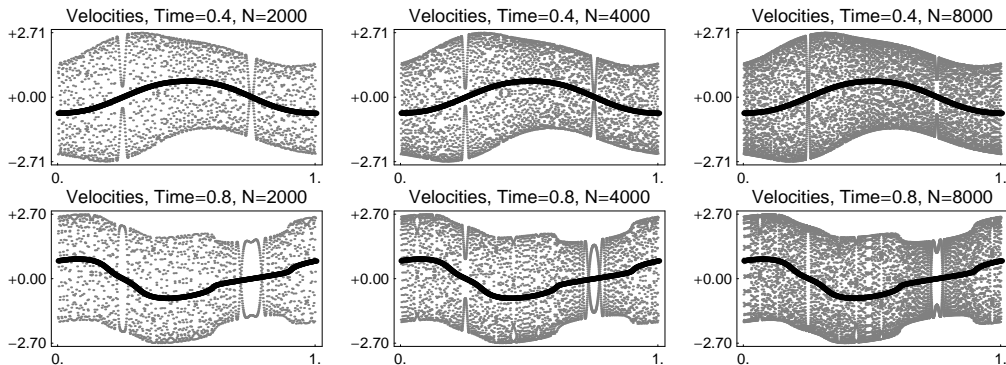


Figure 7. Atomic velocities corresponding to Figure 6. \diamond

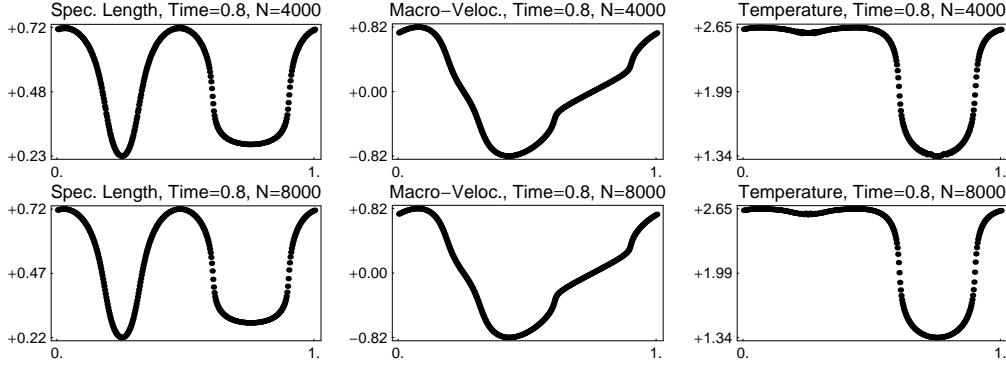


Figure 8. The snapshots of three selected macroscopic fields at $\bar{t} = 0.8$ for $N = 4000$ and $N = 8000$ indicate that the macroscopic fields converge in the sense of functions. \diamond

We have solved Newton's equations with periodic boundary conditions for different particle numbers but within a fixed macroscopic time interval $[0, \bar{t}_{\text{fin}}]$ with $\bar{t}_{\text{fin}} = 0.8$, so that the microscopic final time is $t_{\text{fin}} = N\bar{t}_{\text{fin}}$.

Figures 6 and 7 show snapshots of the resulting atomic distances and velocities, where the data for $N = 2000$, $N = 4000$, and $N = 8000$ are arranged in different columns. The dark colored curves represent the local mean values, i.e., the fields of mean distance and mean velocity, whose computation is described in §3. We observe that the atomic data are highly oscillating on the microscopic scale, and that the oscillations are bounded by sharp envelopes. From the mathematical point of view the oscillations prevent that the limit $N \rightarrow \infty$ can be described completely in terms of functions, and hence any appropriate mathematical descriptions must rely on measures. Even if we are interested in the macroscopic quantities only, the oscillations remain important because some amount of the macroscopic energy is stored in the oscillations. In Figures

N	=	4000/8000		
ma_final_time	=	8.0E-01	mi_final_time	= 3.2E+03/6.4E+03
mi_time_delta	=	1.25E-02	mi_time_steps	= 256000/512000
mv_win_t_len	=	4047/5724	mv_win_p_len	= 20/20
df_win_t_len	=	4047/5724	df_win_p_len	= 40/80
df_win_prm	=	100		

Table 4

Numerical parameters for Example S1. \diamond

6 and 7 we observe the same microscopic oscillations for all particles numbers. For this reason we expect that the atomic data converge as $N \rightarrow \infty$ in the sense of Young measures to a unique limit measure, and this implies that the local mean values converge in the sense of functions, see Figure 8.

The computation of wave number and frequency is illustrated in Figure 9, which shows snapshots of the auxiliary observables Ψ_k and Ψ_ω at $\bar{t} = 0.8$. Again we find strong oscillations in the atomic data, which converge as $N \rightarrow \infty$ in the sense of measures. Moreover, the local mean values converge to

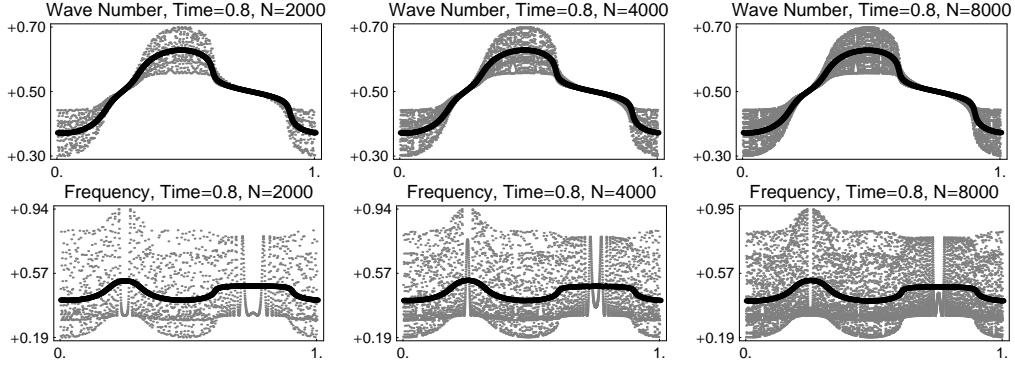


Figure 9. Example $S1$. The local mean values of the oscillating auxiliary observables Ψ_k and Ψ_ω determine the fields of wave number k and frequency ω . The three columns correspond to $N = 2000$, $N = 4000$, and $N = 8000$, respectively. \diamond

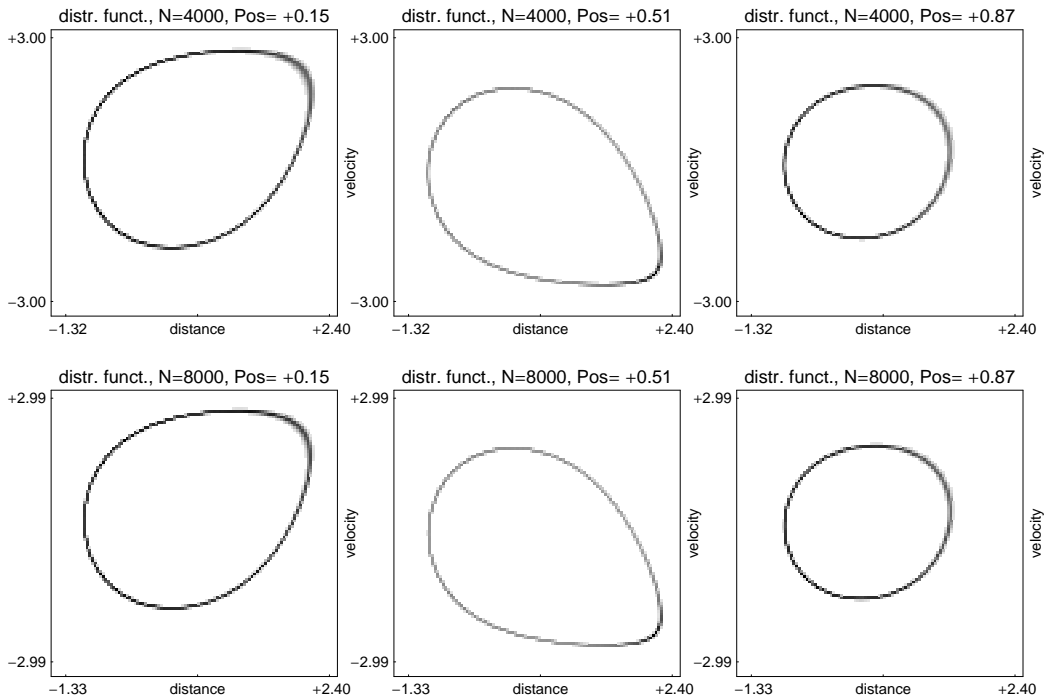


Figure 10. Local distribution functions for Example $S1$ with $N = 4000$ (top) and $N = 8000$ (bottom) in three selected points at $\bar{t} = 0.8$, compare with Figure 11. For large N , the local distribution functions become independent of N and the details of the mesoscopic averaging. \diamond

macroscopic functions, and provide the fields of wave number and frequency.

In a next step we compare the microscopic distribution functions with their macroscopic predictions coming from modulation theory. To this end we fix eight mesoscopic space-time windows. Recall that each of these window contains a lot of time steps and particles, but shrinks to a single point on the macroscopic scale. The mesoscopic windows for this example are located at $\bar{t} = 0.8$ but have different $\bar{\alpha}$ -coordinates, see the bottom right picture in Figure

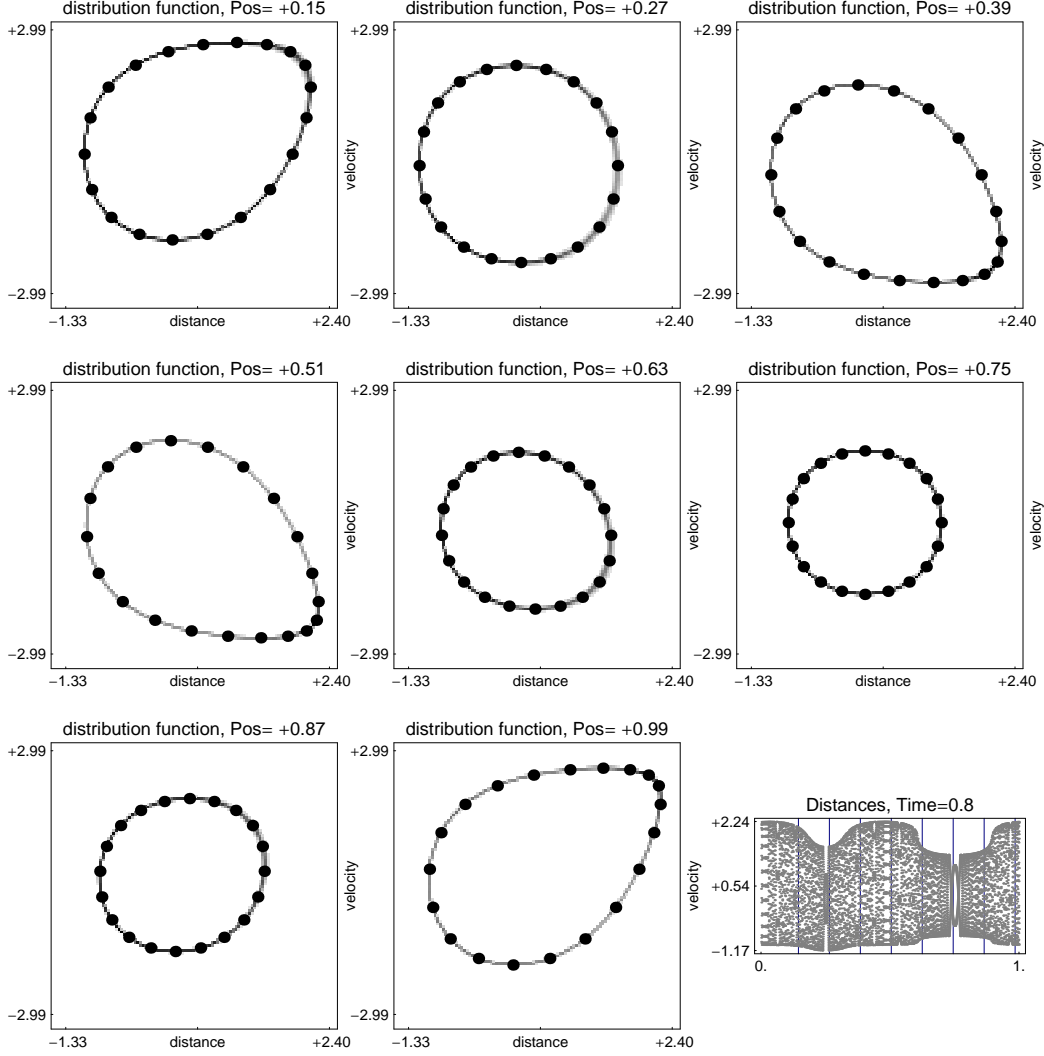


Figure 11. Local distribution functions (White and Gray) and macroscopic predictions (black points) for Example $S1$ with $N = 8000$ in eight selected points at $\bar{t} = 0.8$; for the $\bar{\alpha}$ -coordinates see the vertical lines in the bottom right picture. \diamond

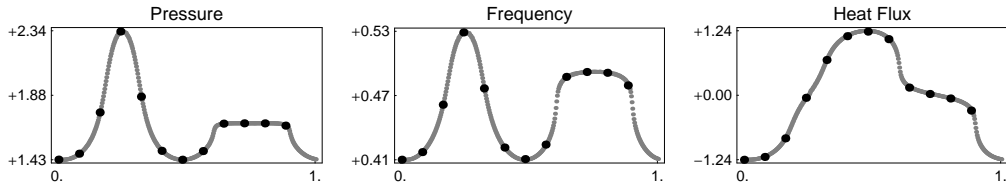


Figure 12. Example $S1$. Comparison between macroscopic fields (Gray) and corresponding TW-fields (Black) for $N = 8000$ and $\bar{t} = 0.8$. \diamond

11. For each window we compute the distribution function of atomic distances and velocities as it is described in §3. This gives rise to the density plots within Figures 10 and 11, where Gray and White indicate a high resp. low probability for finding a particle. Note that (i) the support of every distribution function is contained in a closed curve, and (ii) the distribution functions

vary on the macroscopic scale. Moreover, Figures 10 illustrates that for large N the distribution functions become independent of N .

The black drawn points in Figure 11 represent the macroscopic predictions, and are obtained as follows. Let any window \mathcal{F} be fixed. The values $r_{\mathcal{F}}$, $v_{\mathcal{F}}$, $k_{\mathcal{F}}$ and $T_{\mathcal{F}}$ determine an exact traveling wave with profiles functions $\mathbb{R}_{\mathcal{F}}$ and $\mathbb{V}_{\mathcal{F}}$, and these functions encode all macroscopic predictions concerning the microscopic oscillations. In fact, the microscopic distribution function is predicted to equal the measure of the traveling wave, that is the measure generated by the curve

$$\varphi \mapsto Q^{\text{TW}}(\varphi) = (r_{\mathcal{F}} + \mathbb{R}_{\mathcal{F}}(\varphi + k_{\mathcal{F}}/2), v_{\mathcal{F}} + \omega_{\mathcal{F}} \mathbb{V}_{\mathcal{F}}(\varphi)), \quad (38)$$

see formula (28) in §2.2. In particular, the support of the microscopic distribution within \mathcal{F} is predicted to equal the characteristic trace of the traveling wave, that is the image of the curve (38). To test the validity of the predictions we have computed 24 points $Q_i^{\text{TW}} = Q^{\text{TW}}(\varphi_i)$ of the curve (38) with $\varphi_i = i/20$, $i = 1 \dots 20$. Finally, we have drawn the points Q_i with black color into the density plots of Figure 11.

The eight plots of Figure 11 show that the image of the curve (38) coincides with the support of the microscopic distribution function. Moreover, a closer look to the distribution functions reveals that the distance between adjacent points Q_{i+1} and Q_i is inversely related to the amount of particles located in between these points, see for instance the density plots for $\bar{\alpha} = 0.51$. This implies that all density plots provide the correct height function. From these two observations we conclude that the microscopic oscillations within any window \mathcal{F} can in fact be described by a traveling waves with parameters $r_{\mathcal{F}}$, $v_{\mathcal{F}}$, $k_{\mathcal{F}}$ and $T_{\mathcal{F}}$, and this implies that the atomic data behave like in a modulated traveling waves. Finally, according to the discussion in §3.4 we conclude that the macroscopic dynamics of the thermodynamics fields is governed by the modulation equations (6).

In Figure 12 we compare three macroscopic fields with their corresponding TW-fields, where the TW-fields are plotted in only 25 points. Recall that there is fundamental difference between fields and TW-fields. The fields result immediately from the atomic data by averaging the oscillations. On the other side, TW-fields represent mean values of traveling waves, and thus they depend only on the four macroscopic fields r , v , k and T . In Figure 12 we observe a very good correspondence between fields and TW-fields, and this gives a further confirmation for the validity of modulation theory.

We conclude with a remark. The modulation equations for the harmonic chain, see (31), split into two independent subsystems. Consequently, if we initialize the harmonic chain with the initial data (37), then both wave number k and temperature T will remain constant for all times. The current example

illustrates that for nonlinear chains all four modulation equations are coupled.

Example S2

Here we study the evolution of smooth initial data for a non-integrable interaction potential. To this end we add a fourth order correction to the Toda potential, and obtain

$$\Phi(r) = \exp((1-r)) - (1-r) + \frac{1}{40}(r-1)^4. \quad (39)$$

The initial data, cf. Figure 13, are given by $v^{\text{odd}}(\bar{\alpha}) = v^{\text{even}}(\bar{\alpha}) = 0$ and

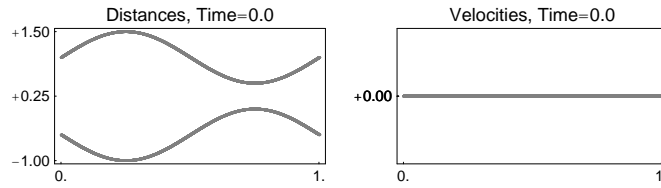


Figure 13. Modulated atomic initial data for Example S2. \diamond

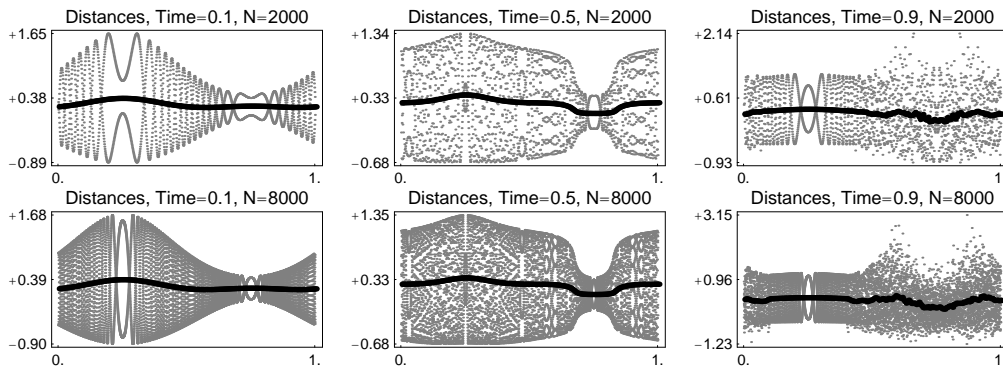


Figure 14. Example S2. Snapshots of the atomic distances. Top and bottom row correspond to $N = 2000$ and $N = 8000$, respectively. The dark colored functions represent the local mean values. \diamond

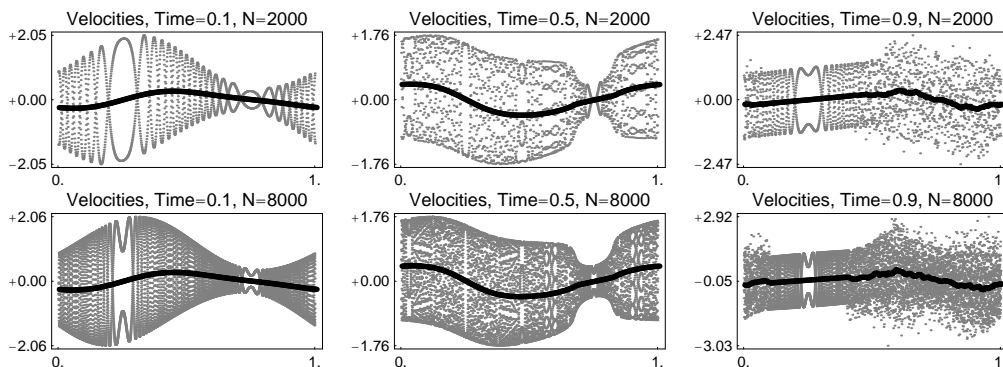


Figure 15. Atomic velocities corresponding to Figure 14. \diamond

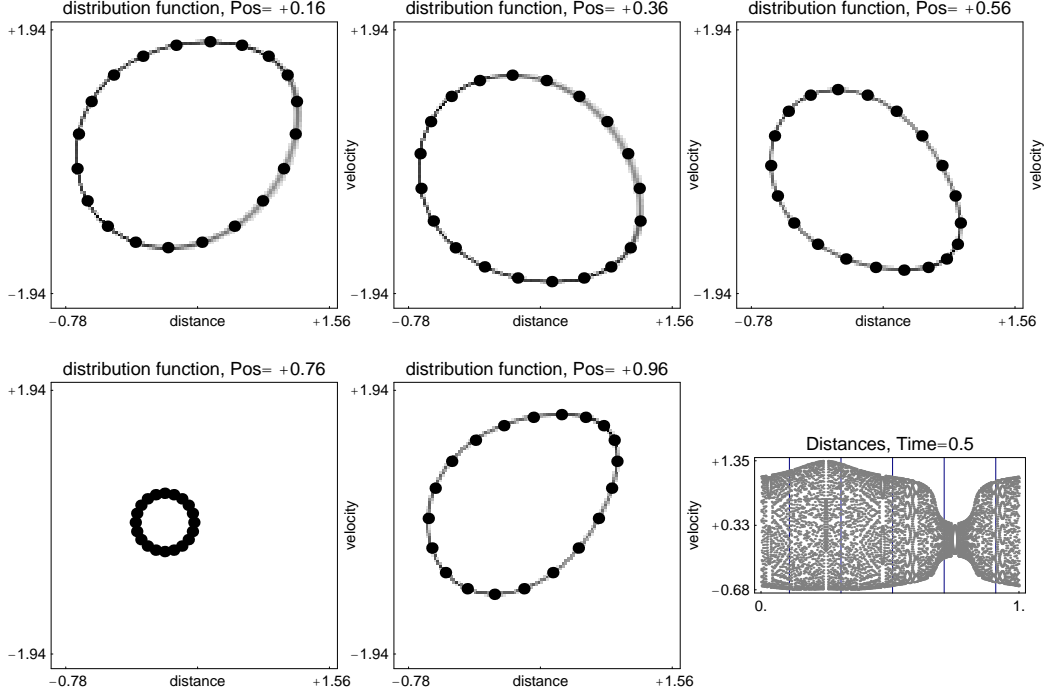


Figure 16. Local distribution functions for Example $S2$ with $N = 8000$ in five selected points at $\bar{t} = 0.5$; the $\bar{\alpha}$ -coordinates are marked by the vertical lines in the bottom right picture. Gray and Black correspond to microscopic distribution functions and macroscopic predictions, respectively. **Interpretation.** For $\bar{t} < 0.5$ all microscopic oscillations take the form of modulated traveling waves. \diamond

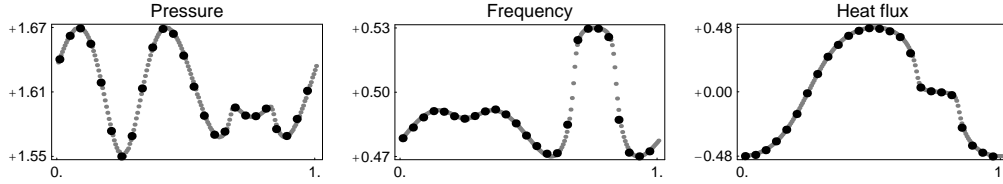


Figure 17. Example $S2$. Comparison between macroscopic fields (Gray) and corresponding TW-fields (Black) with $N = 8000$ and $\bar{t} = 0.5$. \diamond

N	$= 2000/8000$	$mi_final_time = 1.8E+03/7.2E+03$
ma_final_time	$= 0.9E+00$	$mi_time_steps = 90000/360000$
mi_time_delta	$= 2.0E-02$	
$mv_win_t_len$	$= 2236/4472$	$mv_win_p_len = 10/40$
$df_win_t_len$	$= 2236/4472$	$df_win_p_len = 40/89$
df_win_prm	$= 100$	

Table 5

Numerical parameters for Example $S2$. \diamond

$$r^{\text{odd}}(\bar{\alpha}) = 1 + \frac{1}{2} \sin(2\pi\bar{\alpha}), \quad r^{\text{even}}(\bar{\alpha}) = -\frac{1}{2} - \frac{1}{2} \sin(2\pi\bar{\alpha}).$$

While the fields r , v and k are initially constant, we modulate the internal energy U , and this implies a modulation of frequency ω and entropy S . The numerical solution to Newton's equation is shown within Figures 14 and 15, which contain snapshots for $N = 2000$, $N = 8000$ at $\bar{t} = 0.1$, $\bar{t} = 0.5$, and

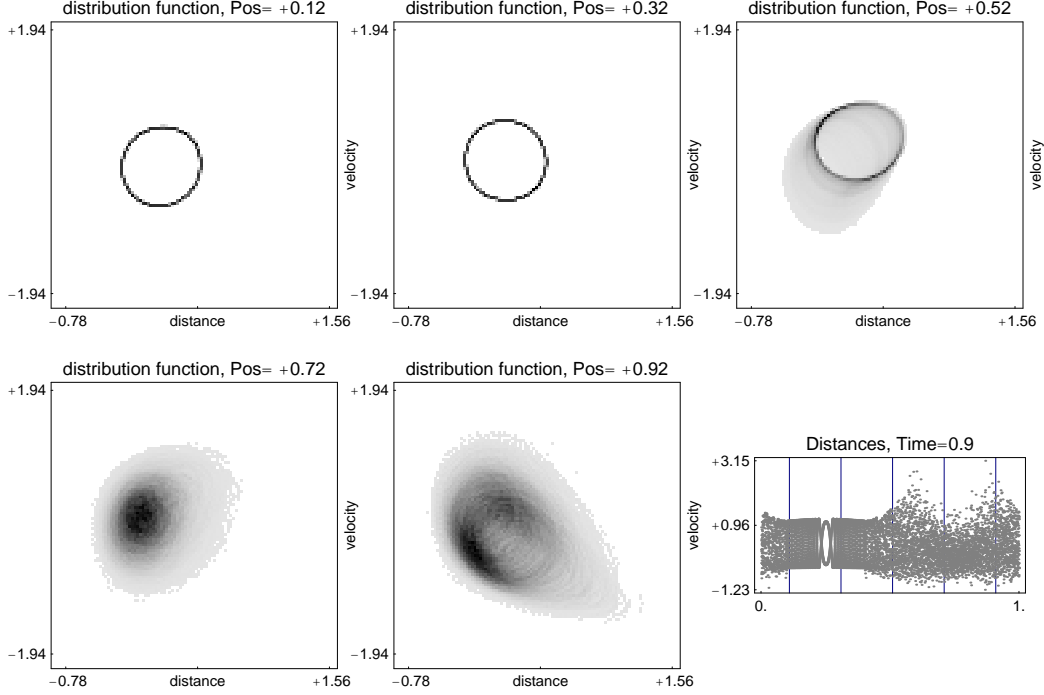


Figure 18. Local distribution functions for Example $S2$ with $N = 8000$ in five selected points at $\bar{t} = 0.9$; for the $\bar{\alpha}$ -coordinates see the vertical lines in the bottom right picture. Gray and Black correspond to microscopic distribution functions and macroscopic predictions, respectively. **Interpretation.** The microscopic oscillations beyond the shock exhibit a more complicate structure, and cannot be described by modulated traveling waves. \diamond

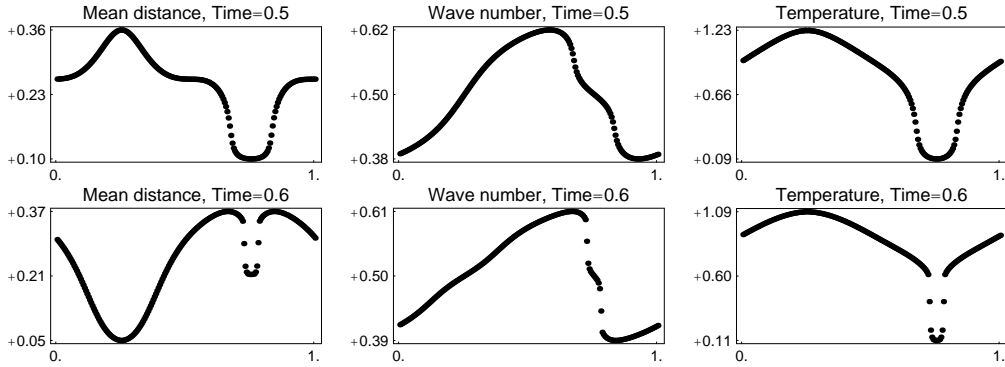


Figure 19. Example $S2$. The formation of macroscopic shocks with $N = 8000$. \diamond
 $\bar{t} = 0.9$.

For macroscopic times $\bar{t} \approx 0.5$ we observe the same qualitative behavior as in Example $S1$. The atomic data converge for $N \rightarrow \infty$ to a Young measure, and the local mean values converge in the sense of functions. Furthermore, the atomic oscillations are again bounded by sharp envelopes. In Figure 16 we compare the microscopic distribution functions with their macroscopic predictions in eight selected points at $\bar{t} = 0.5$. As for the previous example we observe

a very good correspondence between microscopic oscillations and macroscopic predictions, and Figure 17 yields a good matching of fields and TW-fields.

At $\bar{t} = 0.9$ we can identify a region, namely $0.4 \lesssim \bar{\alpha} \lesssim 1.1$, where the microscopic oscillations exhibit a different behavior. According to Figure 18 the support of the microscopic distribution functions are not contained in closed curves anymore, but fill a set with positive measure. We conclude, that the microscopic oscillations in this region cannot be described by modulated traveling waves. Figure 19 provides an explanation for this observation. As $\bar{t} \rightarrow 0.6$ the gradients of all fields become steeper and steeper, so that finally at $\bar{t} \approx 0.6$ two shocks are formed. These shocks, which arise from data with temperature, are the reason that modulation theory with periodic traveling waves cannot capture the microscopic oscillations for $\bar{t} \gtrsim 0.6$. For integrable systems like the Toda chain it is known, cf. [BY92,DM98,EI05], that the oscillations beyond such shocks can be described in terms of modulated two-phase traveling waves, but a similar theory for non-integrable system is not yet available.

Example S3

In this example we initialize a periodic chain with *cold* but smooth initial data. The potential is $\Phi(r) = \cosh(r - 1)$, and the initial data are given by $r_\alpha(0) = r_{\text{ini}}(\varepsilon\alpha)$ and $v_\alpha(0) = v_{\text{ini}}(\varepsilon\alpha)$ with

$$r_{\text{ini}}(\bar{\alpha}) = 3.5, \quad v_{\text{ini}}(\bar{\alpha}) = 2.75 \sin(2\pi\bar{\alpha}) + 2.75 \cos(4\pi\bar{\alpha}).$$

Two corresponding solutions to Newton's equations are shown in Figures 20

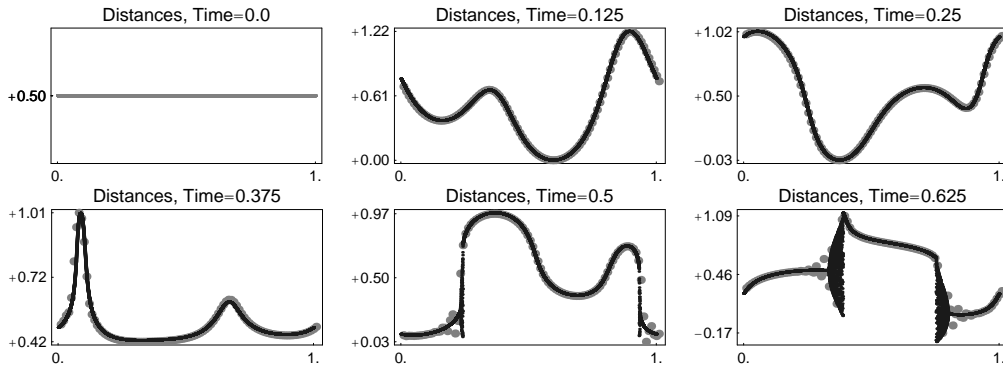


Figure 20. Example S3. Snapshots of the atomic distances. For several macroscopic times \bar{t} the data are plotted against $\bar{\alpha}$. Bright and dark correspond to $N = 100$ and $N = 8000$, respectively. At $\bar{t} \approx 0.5$ the atomic data start to oscillate on the microscopic scale, and temperature is created. \diamond

and 21, where bright and dark colored points correspond to $N = 100$ and $N = 8000$, respectively.

For $\bar{t} \gtrsim 0.1$ the numerical simulations provide evidence that the atomic data

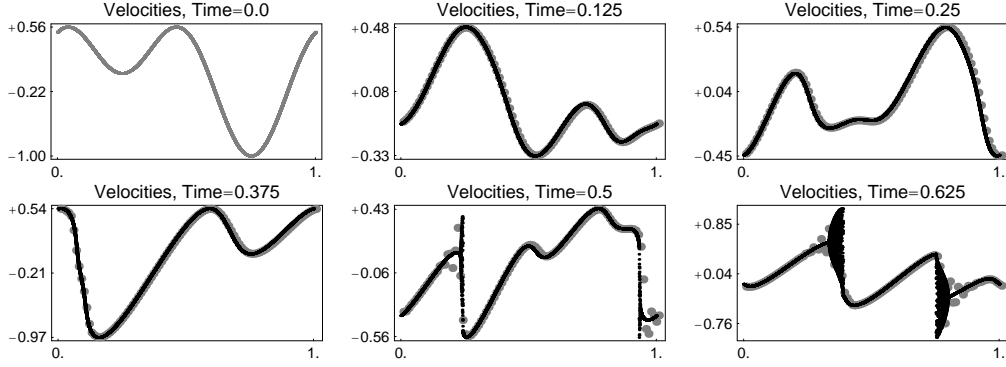


Figure 21. Atomic velocities corresponding to Figure 20. \diamond

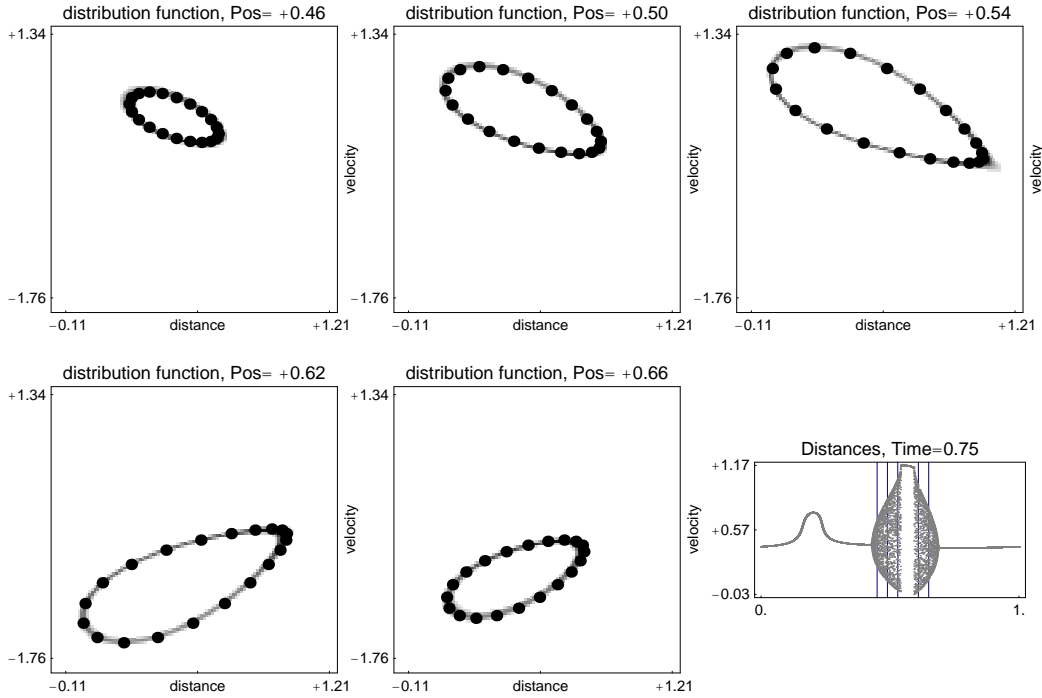


Figure 22. Local distribution functions for Example $S3$ with $N = 8000$ in five selected points at $\bar{t} = 0.18$; the $\bar{\alpha}$ -coordinates are marked by the vertical lines in the bottom right picture. Gray and Black correspond to microscopic distribution functions and macroscopic predictions, respectively. **Interpretation.** The atomic data beyond a cold shock self-organize into modulated traveling waves. \diamond

remain cold, and converge as $N \rightarrow \infty$ to *smooth macroscopic functions*, so that in each point $(\bar{t}, \bar{\alpha})$ we find unique limit values $r(\bar{t}, \bar{\alpha})$ and $v(\bar{t}, \bar{\alpha})$ for the atomic distances and velocities, respectively. In particular, the cold limit functions r and v must satisfy the ansatz (11), and we conclude that the macroscopic evolution of r and v is governed by the nonlinear string system (12). Of course, this is only a numerical observation, but we mention that for a similar model the convergence to smooth and cold limit data was proved in [GL88] by exploiting Strang's Theorem [Str64].

At time $\bar{t} \approx 0.1$ the smooth macroscopic fields r and v form a shock, and the atomic data start to oscillate beyond this shock. As before, these oscillations give rise to a nonvanishing temperature field on the macroscopic scale. Recall that for $\bar{t} > 0.1$ the system (12) is not longer an appropriate model for the macroscopic evolution as it does not conserve mass, momentum, *and* energy beyond the shock.

N	=	100/8000		
ma_final_time	=	1.8E-01	mi_final_time	= 1.8E+01/1.44E03
mi_time_delta	=	5.0E-03	mi_time_steps	= 3600/288000
mv_win_t_len	=	398/3219	mv_win_p_len	= 1/40
df_win_t_len	=	1265/3219	df_win_p_len	= 1/40
df_win_prm	=	100		

Table 6

Numerical parameters for Example *S3*. \diamond

Next we investigate the fine-structure of the microscopic oscillations within the region with temperature by comparing the microscopic distribution functions with their macroscopic predictions in five selected points at $\bar{t} = 0.18$, see Figure 22. Again we observe a good correspondence between microscopic distribution functions and macroscopic predictions, and we conclude that in this example the oscillations can in fact be described by modulated traveling waves. For further details on cold shocks we refer to Example *R1*.

Example *S4*

In all previous simulations the interaction potential Φ was a convex function. The current example shows that this restriction is essential. We consider the double-well potential

$$\Phi(r) = +2 \cosh(2 - r) - \sinh(1)(r - 2)^2,$$

which is concave in the vicinity of its unstable equilibrium at $r = 2$. At time

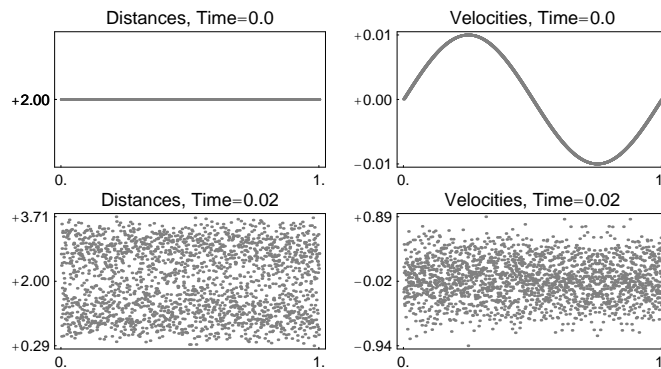


Figure 23. Example *S4*. Snapshots of the atomic distances and velocities at $\bar{t} = 0.0$ and $\bar{t} = 0.02$. \diamond

$\bar{t} = 0$ we impose the cold initial data

$$r^{\text{odd}}(\bar{\alpha}) = r^{\text{even}}(\bar{\alpha}) = 2, \quad v^{\text{odd}}(\bar{\alpha}) = v^{\text{even}}(\bar{\alpha}) = \frac{1}{10} \cos(2\pi\bar{\alpha}),$$

so that the evolution starts in the region of concavity of Φ . In Figure 23 we

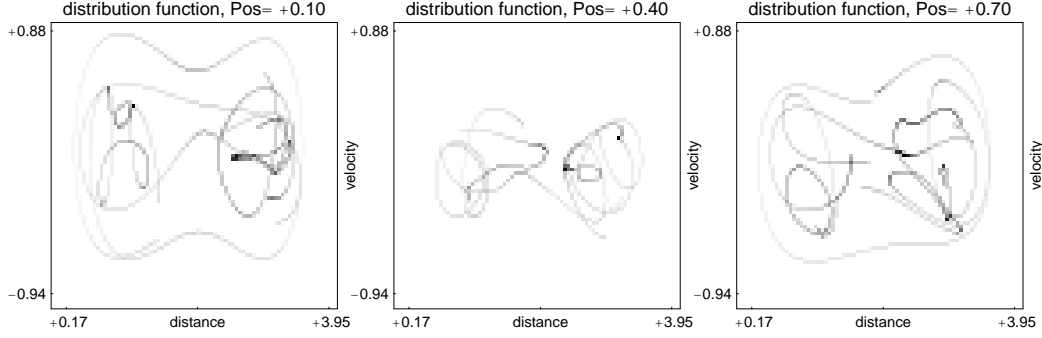


Figure 24. Microscopic distribution functions for Example *S4* in three selected points at $\bar{t} = 0.02$. **Interpretation.** Since Φ is non-convex, the arising microscopic oscillations cannot be described by modulated traveling waves. \diamond

N	=	2000		
ma_final_time	=	2.0E-02	mi_final_time	= 4.0E+01
mi_time_delta	=	2.5E-03	mi_time_steps	= 16000
df_win_t_len	=	4000	df_win_p_len	= 5
df_win_prm	=	75		

Table 7

Numerical parameters for Example *S4*. \diamond

observe that the cold initial data immediately generate temperature, but the corresponding oscillations cannot be described by modulated traveling waves as they exhibit a completely different structure, see Figure 24. In particular, the supports of the distribution functions are not contained in closed curves, and this corresponds to the absence of sharp envelopes in Figure 23. These results are not surprising at all, because the nonlinear string system (12) is not hyperbolic for non-convex interaction potentials Φ (in the regions of concavity it is elliptic). Recall that here we start in the region with concave potential. In case that all initial distances are chosen sufficiently close to either one of the stable equilibria of Φ , then we expect that the data remain cold until either an atomic distance runs into the region with $\Phi'' < 0$, or the first shock is formed.

5 Simulations to Riemann problems

Example R1

We study the evolution of cold Riemann initial data for an infinite chain with modified Toda potential (39), and initialize the atoms with

$$r^{\text{odd}}(\bar{\alpha}) = r^{\text{even}}(\bar{\alpha}) = \begin{cases} 0 & \text{for } \bar{\alpha} < 0.6, \\ 1 & \text{for } \bar{\alpha} \geq 0.6, \end{cases}$$

and $v^{\text{odd}}(\bar{\alpha}) = v^{\text{even}}(\bar{\alpha}) = 0$. The corresponding numerical solutions for $N =$

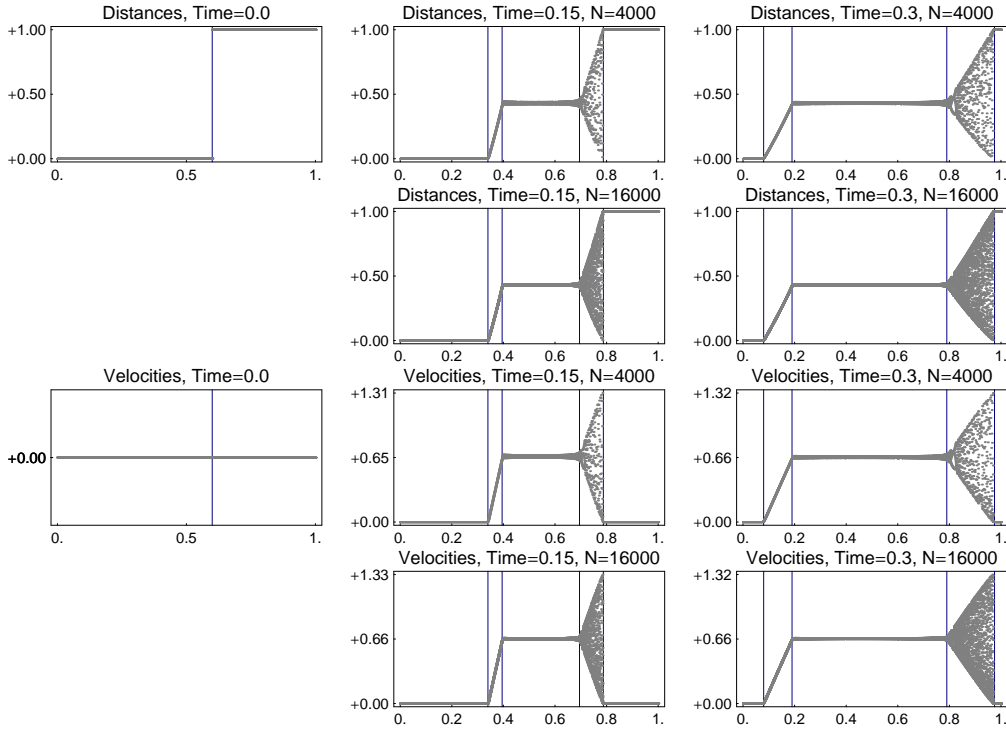


Figure 25. Example R1. Snapshots of atomic distances and velocities at $\bar{t} = 0.0$, $\bar{t} = 0.15$, and $\bar{t} = 0.3$, for $N = 4000$ and $N = 16000$. The vertical lines separate waves from constant states. \diamond

4000 and $N = 16000$ are depicted in Figure 25, and allow for the following interpretations.

- (1) There is a cold rarefaction wave running to the left.
- (2) We find a second, right going wave, which has a head and a rear front. Within this wave the motion generates microscopic oscillations but there are no oscillations outside this wave.
- (3) Between the two waves we observe a new constant state with cold data.
- (4) The macroscopic behavior is independent of the particle number.

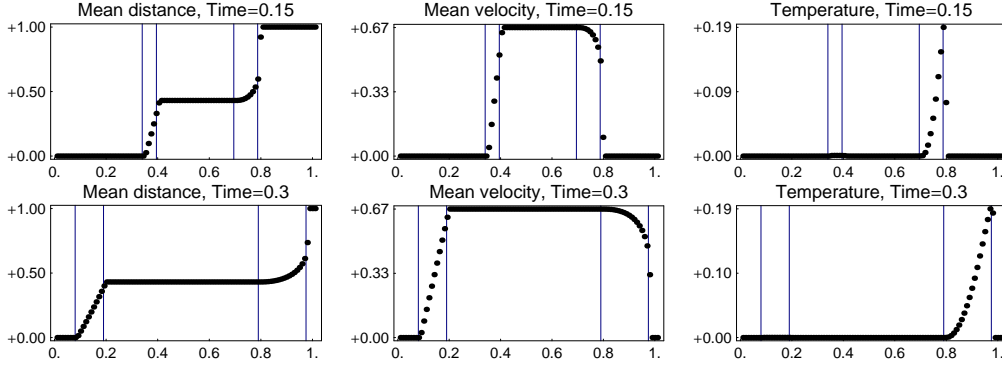


Figure 26. Example *R1*. Snapshots of various macroscopic fields at $\bar{t} = 0.15$ and $\bar{t} = 0.3$ for $N = 16000$. Vertical lines again separate waves from constant states. \diamond

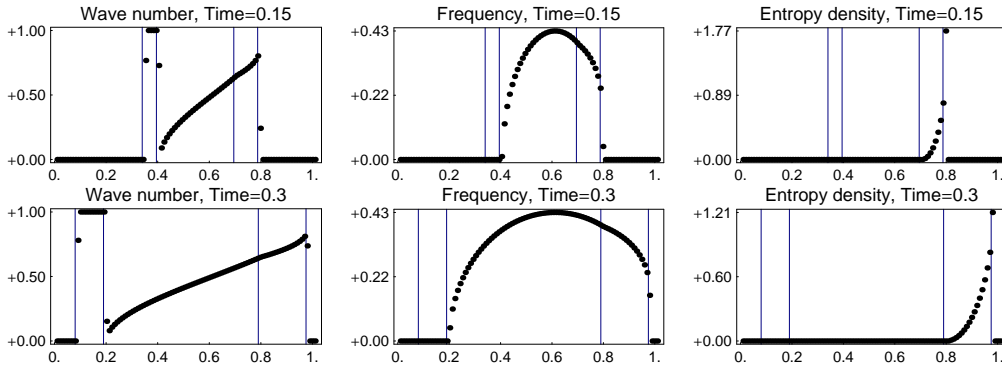


Figure 27. see Figure 26. \diamond

<code>N</code>	<code>= 4000/16000</code>	<code>mi_final_time = 1.2E+03/4.8E+03</code>
<code>ma_final_time</code>	<code>= 3.0E-01</code>	<code>mi_time_steps = 120000/480000</code>
<code>mi_time_delta</code>	<code>= 1.0E-02</code>	<code>mv_win_p_len = 40/126</code>
<code>mv_win_t_len</code>	<code>= 1879/3794</code>	<code>df_win_p_len = 40/126</code>
<code>df_win_t_len</code>	<code>= 1879/3794</code>	
<code>df_win_prm</code>	<code>= 100</code>	

Table 8

Numerical parameters for Example *R1*. \diamond

Note that our concept of waves follows the theory of hyperbolic PDEs, i.e., each wave connects two constant states. In particular, we interpret the region with temperature as a single wave with head and rear front. In §1 we have argued that the onset of microscopic oscillations is caused by the conservation of mass, momentum, and energy, which prevents that the microscopic data beyond a cold shock remain cold. Since the same qualitative behavior is typical for zero dispersion limits we will refer to the second wave as a *dispersive shock wave*.

Figures 26 and 27 show various macroscopic fields, which all exhibit a self-similar profile, i.e., they depend only on $\bar{c} := (\bar{\alpha} - 0.6)/\bar{t}$. The temperature within the constant intermediate state vanishes, and hence both wave number k and frequency ω have no physical meaning here. However, the values we observe for k and ω have some reasonable explanation. Since they are produced by very small oscillations they satisfy the dispersion relation as well as the

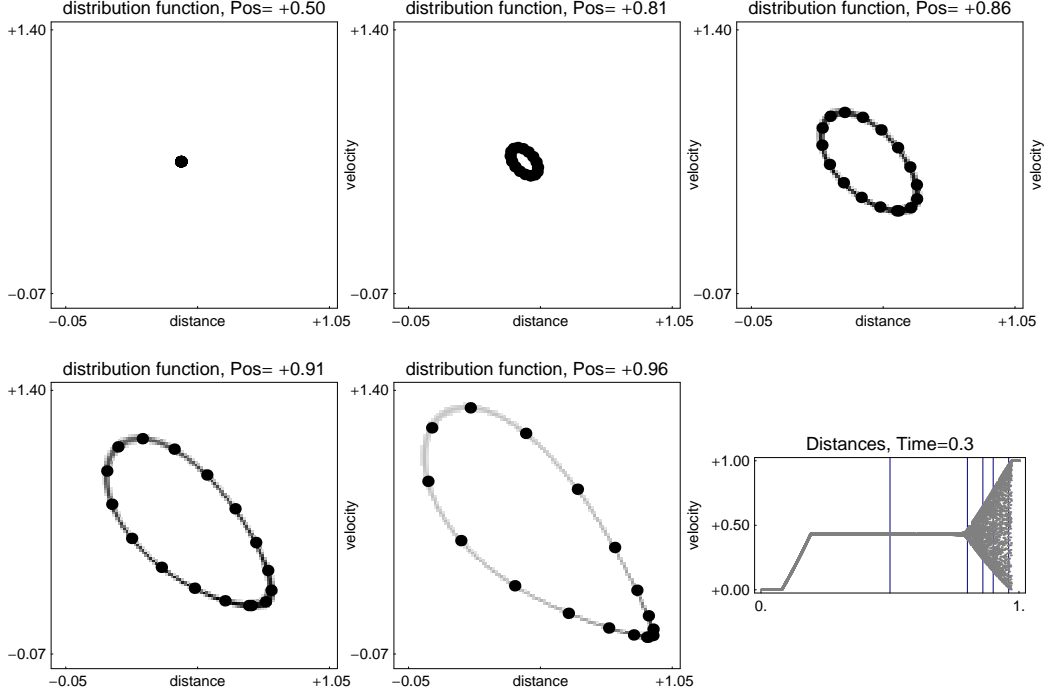


Figure 28. Local distribution functions for Example *R1* in five selected points at $\bar{t} = 0.3$ for $N = 16000$. The $\bar{\alpha}$ -coordinates of the mesoscopic windows are marked by the vertical lines in the bottom right picture. Gray and Black correspond to microscopic distribution functions and macroscopic predictions, respectively. \diamond

evolution equation for k from the harmonic theory, see §2.4.

Figures 26 and 27 seem to indicate that every macroscopic field jumps at the head front of the dispersive wave. However, our simulations do not allow for a definite decision whether all fields remain discontinuous when we increase the number of particles further. In fact, formal arguments developed in [DHR06,HR07] provide some indications that only the entropy density is discontinuous for $N \rightarrow \infty$, whereas all other fields, especially the temperature, become continuous but have infinite derivative. Here we focus on the microscopic oscillations within the dispersive wave, and postpone a detailed investigation of the vicinity of the head front to future research.

In Figure 28 we compare the microscopic distribution functions with their macroscopic predictions in five selected points at $\bar{t} = 0.3$. Again we observe a good coincidence between microscopic distribution functions and macroscopic predictions. Thus we conclude that the microscopic oscillations take in fact the form of a modulated traveling wave. As mentioned in the introduction, there is an elaborated theory for Riemann problems in the Toda chain, but all these results do not address the qualitative behavior of the generic thermodynamic fields.

Example R2

In this example we study the contact problem between a cold state and a binary oscillation for the Toda chain, and choose $v^{\text{odd}}(\bar{\alpha}) = v^{\text{even}}(\bar{\alpha}) = 0$ and

$$r^{\text{odd}}(\bar{\alpha}) = \begin{cases} -1 & \text{for } \bar{\alpha} < 0.5, \\ +1 & \text{for } \bar{\alpha} \geq 0.5, \end{cases} \quad r^{\text{even}}(\bar{\alpha}) = \begin{cases} +3 & \text{for } \bar{\alpha} < 0.5, \\ +1 & \text{for } \bar{\alpha} \geq 0.5. \end{cases}$$

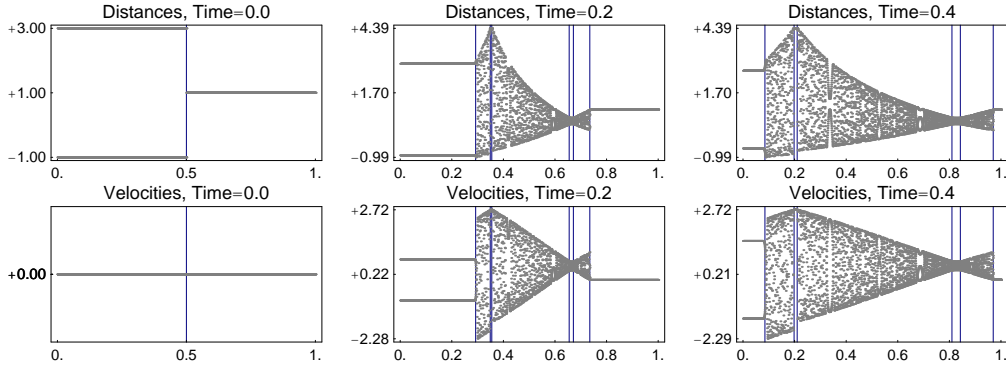


Figure 29. Example *R2*. Snapshots of atomic distances and velocities at $\bar{t} = 0.0$, $\bar{t} = 0.2$, and $\bar{t} = 0.4$. The vertical lines separate waves from constant states. \diamond

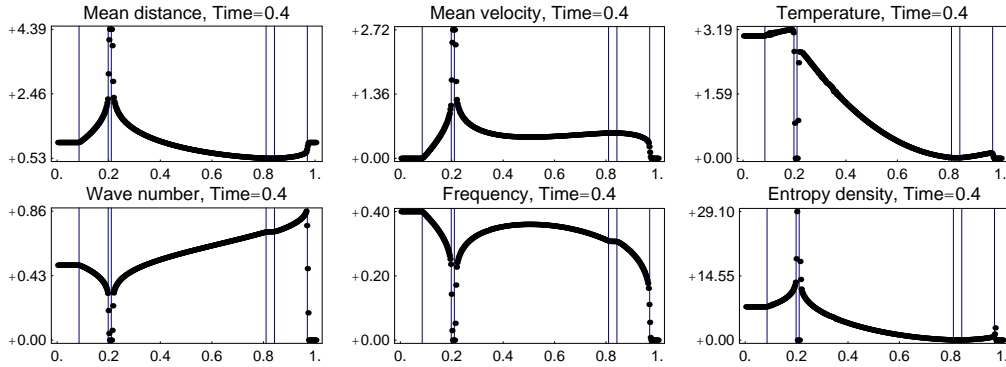


Figure 30. Example *R2*. Snapshots of selected macroscopic fields at $\bar{t} = 0.4$. \diamond

N	=	4000		
ma_final_time	=	4.0E-01	mi_final_time	= 1.6E+03
mi_time_delta	=	1.0E-02	mi_time_steps	= 160000
mv_win_t_len	=	2529	mv_win_p_len	= 10
df_win_t_len	=	2529	df_win_p_len	= 20
df_win_prm	=	100		

Table 9

Numerical parameters for Example *R2*. \diamond

Figure 29 shows the atomic data for $N = 4000$ at $\bar{t} = 0.0$, $\bar{t} = 0.2$, and $\bar{t} = 0.4$, and Figure 30 contains snapshots of various macroscopic fields. We observe the

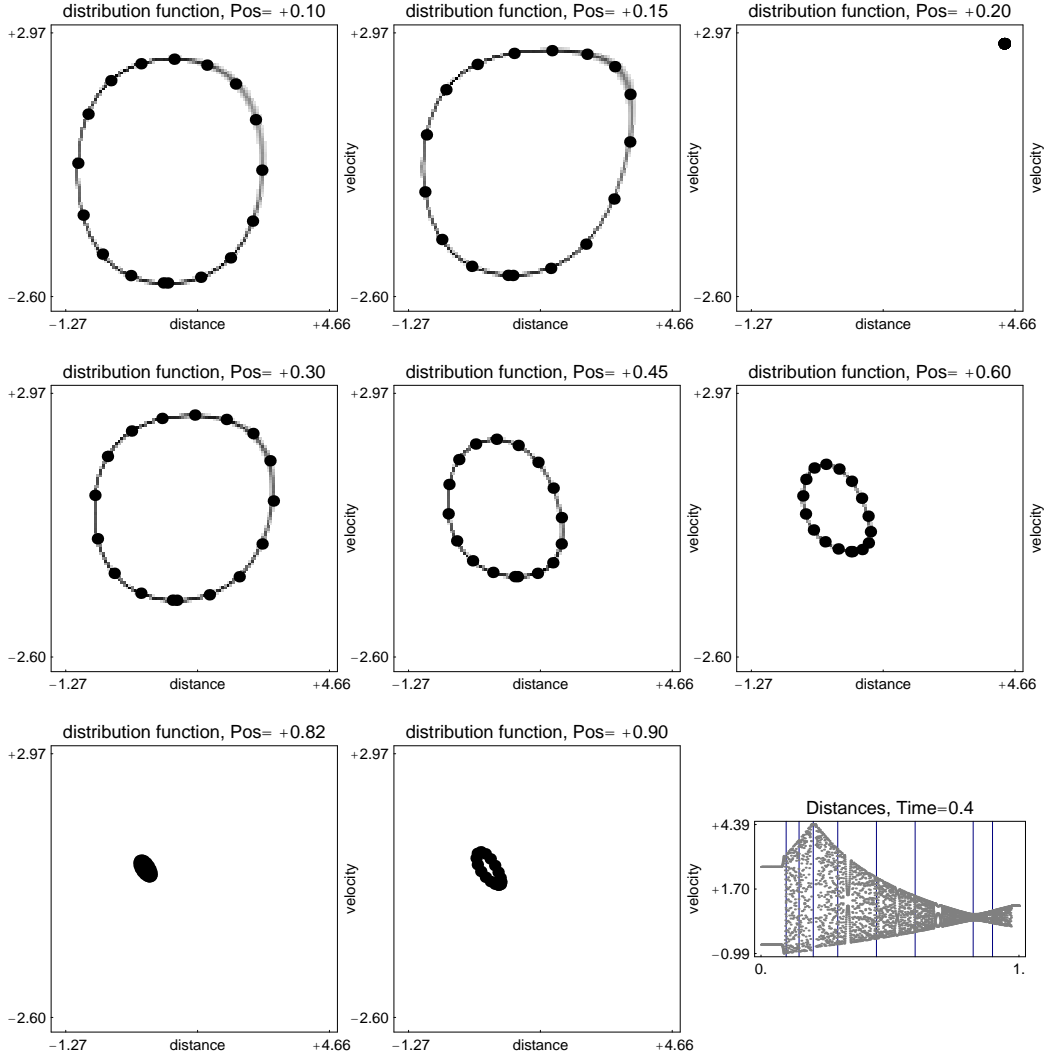


Figure 31. Local distribution functions for Example $R2$ in eight selected points at $\bar{t} = 0.4$; the $\bar{\alpha}$ -coordinates are marked by the vertical lines in the bottom right picture. Gray and Black correspond to microscopic distribution functions and macroscopic predictions, respectively. \diamond

creation of three self-similar waves having two fronts each. The first wave runs to the left, the second wave spreads out both to the left and to the right, and the third wave goes to the right. All waves are separated by constant states, where the width of the constant state in between the first and second wave is very small.

By construction, the third wave contacts a region with zero temperature. Surprisingly, the same is true for the first two waves because the temperature vanishes in the constant state in between. In particular, the entropy increases with \bar{t} within the first wave, then it jumps to zero, jumps back to a positive value, and finally it decreases with \bar{t} within the second wave. Due to this qualitative behavior we classify all three waves as dispersive shocks.

In Figure 31 we compare the microscopic distribution functions with their macroscopic predictions in eight selected macroscopic points which cover all three waves, and again we find a good matching between the microscopic and the macroscopic predictions. This result is quite surprising as the Riemann initial data are not cold but have temperature.

Example R3

In this example we consider a Riemann-problem for the Toda chain with binary oscillations at both sides of the initial jump. We set $v^{\text{odd}}(\bar{\alpha}) = v^{\text{even}}(\bar{\alpha}) = 0$ and

$$r^{\text{odd}}(\bar{\alpha}) = \begin{cases} 0 & \text{for } \bar{\alpha} < 0.38, \\ 2 & \text{for } \bar{\alpha} \geq 0.38, \end{cases}, \quad r^{\text{even}}(\bar{\alpha}) = \begin{cases} 1 & \text{for } \bar{\alpha} < 0.38, \\ 3 & \text{for } \bar{\alpha} \geq 0.38, \end{cases}$$

so that the initial jump is located at $\bar{\alpha} = 0.38$. The resulting atomic data for

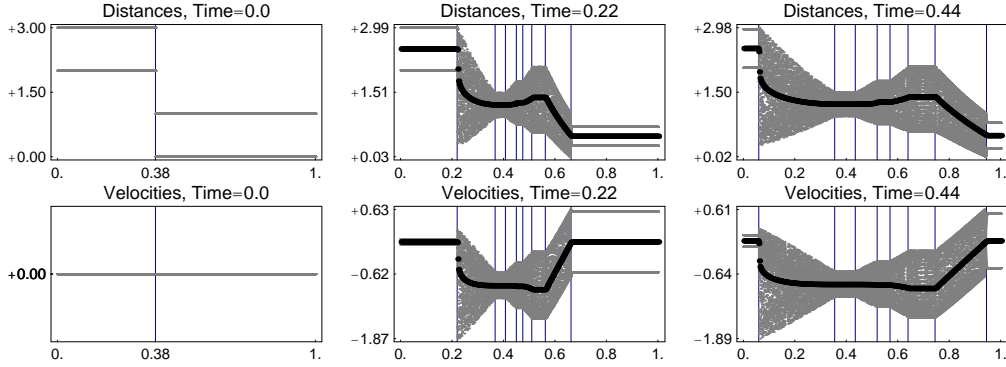


Figure 32. Example R3. Atomic distances and velocities at $\bar{t} = 0.0$, $\bar{t} = 0.22$ and $\bar{t} = 0.44$. The vertical lines separate waves from constant states. \diamond

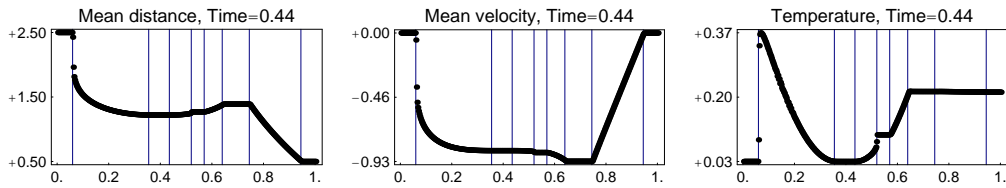


Figure 33. Example R3. Snapshots of several macroscopic fields at $\bar{t} = 0.44$. \diamond

N	=	16000		
ma_final_time	=	4.4E-01	mi_final_time	= 7.04E+03
mi_time_delta	=	2.0E-02	mi_time_steps	= 352000
mv_win_t_len	=	2782	mv_win_p_len	= 40
df_win_t_len	=	475	df_win_p_len	= 1
df_win_prm	=	100		

Table 10

Numerical parameters for Example R3. \diamond

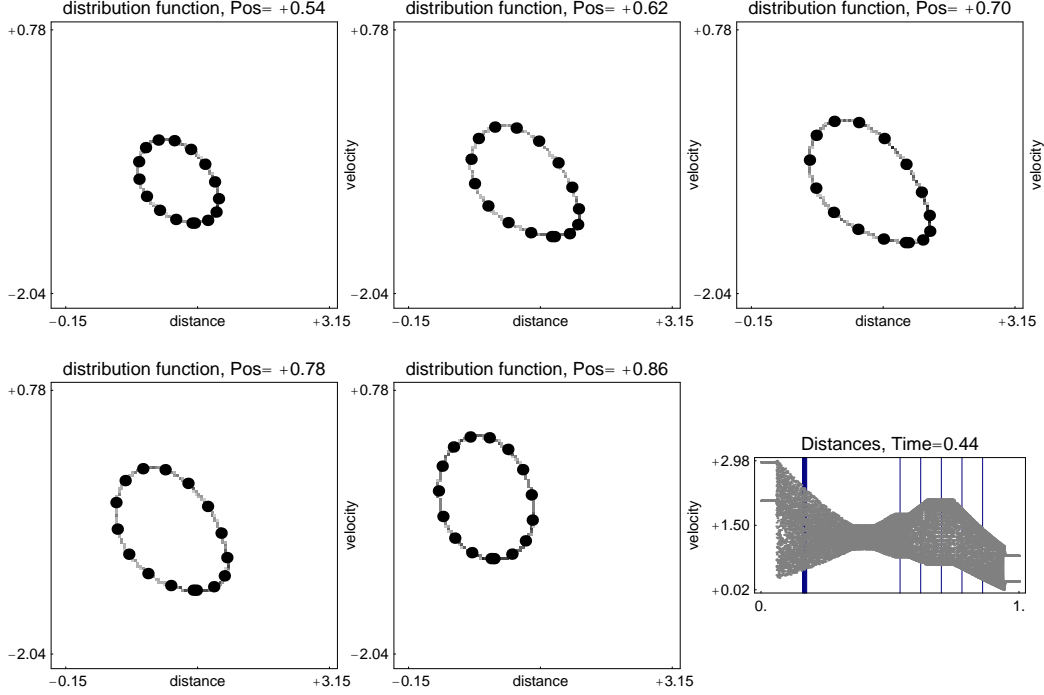


Figure 34. Local distribution functions for Example *R3* in five selected points at $\bar{t} = 0.44$ **right of the second wave**; the $\bar{\alpha}$ -coordinates are marked by the vertical lines in the bottom right picture. Gray and Black correspond to microscopic distribution functions and macroscopic predictions, respectively. **Interpretation.** The microscopic oscillations within this region can be described by modulated traveling waves. \diamond

$N = 16000$ are presented in Figure 32, and Figure 33 contains the profiles of various macroscopic fields. We can identify four consecutive waves, which all are separated by constant states.

At first we study the third and the fourth wave, which we classify as rarefaction waves. Note that the temperature remains constant within the fourth wave. We choose five macroscopic points right of the second wave, and compare the microscopic distribution functions with their macroscopic predictions. The results are presented in Figure 34. We observe a good matching between microscopic and macroscopic data, and can conclude that the microscopic oscillations within this region are generated by a modulated traveling wave.

The microscopic oscillations within the first two waves cannot be described by modulated traveling waves, and thus modulation theory with periodic traveling waves must fail here. To justify this assertion again we compare microscopic distribution functions with macroscopic predictions, see Figure 35. This comparison is now carried out in nine macroscopic points which all are very close to each other so that the macroscopic predictions almost coincide. In contrast to the preceding examples, here the underlying space-time windows contain only one particle so that all microscopic distribution functions in Figure 35

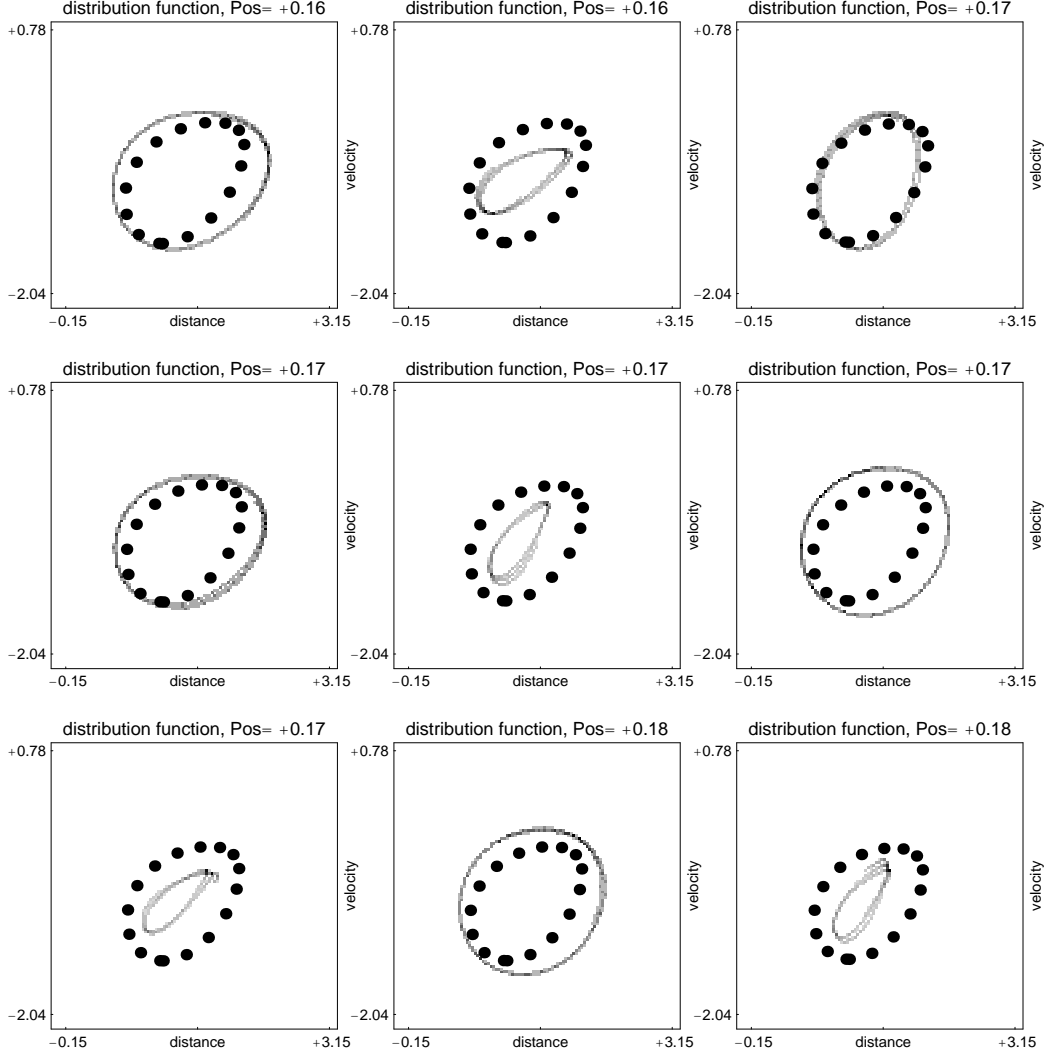


Figure 35. Local distribution functions for Example *R3* in nine selected points in the neighborhood of $(\bar{t} = 0.44, \bar{\alpha} = 0.17)$, compare the bottom right picture in Figure 34. Gray and Black correspond to microscopic distribution functions (for one single particle) and macroscopic predictions, respectively. **Interpretation.** The microscopic distribution functions oscillate around the macroscopic predictions. \diamond

describe the temporal statistics of a single particle. These one-particle distributions do not meet the macroscopic predictions but oscillate around them. We mention that the same behavior can be found within the second wave.

The data from Figure 35 suggest that every one-particle distribution function is still equivalent to a traveling wave. However, these traveling waves now oscillate on the microscopic scale. For harmonic lattices this phenomenon can be understood in terms of Wigner-measures which allow for the fast modulation of wave number and frequency, see [Mac02,Mac04,Mie06]. Unfortunately, no similar concept is presently available for nonlinear system.

Acknowledgements. Research was supported by *Deutsche Forschungsgemeinschaft* (DFG) within the Priority Program SPP 1095 *Analysis, Modeling and Simulation of Multiscale Problems*. We gratefully acknowledge countless fruitful discussions with Alexander Mielke and Jens Rademacher.

References

- [AG96] G. Arioli and F. Gazzola, *Periodic motion of an infinite lattice of particles with nearest neighbor interaction*, Nonl. Anal. TMA **26** (1996), no. 6, 1103–1114.
- [BY92] A.M. Bloch and Y.Kodama, *Dispersive regularization of the Whitham equation for the Toda lattice*, SIAM J. Appl. Math. **52** (1992), no. 4, 909–928.
- [Daf00] C.M. Dafermos, *Hyperbolic conservation laws in continuum physics*, Grundlehren d. mathem. Wissenschaften, vol. 325, Springer, Berlin, 2000.
- [DH05] W. Dreyer and M. Herrmann, *On the approximation of periodic traveling waves for the atomic chain*, WIAS preprint 1030, 2005.
- [DHM06] W. Dreyer, M. Herrmann, and A. Mielke, *Micro-macro transition for the atomic chain via Whitham’s modulation equation*, Nonlinearity **19** (2006), no. 2, 471–500.
- [DHR06] W. Dreyer, M. Herrmann, and J. Rademacher, *Wave trains, solitons and modulation theory in FPU chains*, Analysis, Modeling and Simulation of Multiscale Problems (A. Mielke, ed.), Springer, 2006, To appear.
- [DK00] W. Dreyer and M. Kunik, *Cold, thermal and oscillator closure of the atomic chain*, J. Phys. A: Math. Gen. **33** (2000), 2097–2129.
- [DM98] P. Deift and T. T-R McLaughlin, *A continuum limit of the Toda lattice*, Mem. Americ. Math. Soc., vol. 131/624, American Mathematical Society, 1998.
- [El05] G.A. El, *Resolution of a shock in hyperbolic systems modified by weak dispersion*, Chaos **15** (2005), 037103–14.
- [Fla74] H. Flaschka, *The Toda lattice ii. existence of integrals*, Phys. Rev. B **9** (1974), no. 4, 1924–1925.
- [FM02] G. Friesecke and K. Matthies, *Atomic-scale localization of high-energy solitary waves on lattices*, Physica D **171** (2002), 211–220.
- [FP99] G. Friesecke and R. L. Pego, *Solitary waves on FPU lattices. I. Qualitative properties, renormalization and continuum limit*, Comm. Math. Phys. **12** (1999), no. 6, 1601–1627.

- [FV99] A.-M. Filip and S. Venakides, *Existence and modulation of traveling waves in particle chains*, Comm. Pure Appl. Math. **51** (1999), no. 6, 693–735.
- [FW94] G. Friesecke and J. A. D. Wattis, *Existence theorem for solitary waves on lattices*, Comm. Math. Phys. **161** (1994), no. 2, 391–418.
- [GHM06] J. Giannoulis, M. Herrmann, and A. Mielke, *Continuum descriptions for the dynamics in discrete lattices: derivation and justification*, Analysis, Modeling and Simulation of Multiscale Problems (A. Mielke, ed.), Springer, 2006, To appear.
- [GL88] J. Goodman and P. Lax, *On dispersive difference schemes*, Comm. Pure Appl. Math. **41** (1988), 591–613.
- [GM04] J. Giannoulis and A. Mielke, *The nonlinear Schrödinger equation as a macroscopic limit for an oscillator chain with cubic nonlinearities*, Nonlinearity **17** (2004), 551–565.
- [GM06] J. Giannoulis and A. Mielke, *Dispersive evolution of pulses in oscillator chains with general interaction potentials*, Discr. Cont. Dynam. Systems Ser. B **6** (2006), 493–523.
- [GR96] E. Godlewski and P.-A. Raviart, *Numerical Approximation of Hyperbolic Conservation Laws*, Applied Mathematical Sciences, vol. 118, Springer, Berlin, 1996.
- [Hén74] M. Hénon, *Integrals of the Toda lattice*, Phys. Rev. B **9** (1974), no. 4, 1921–1923.
- [Her05] M. Herrmann, *Ein Mikro-Makro-Übergang für die nichtlineare atomare Kette mit temperatur*, Phd thesis, Humboldt-Universität zu Berlin, 2005.
- [HFM81] B.L. Holian, H. Flaschka, and D.W. McLaughlin, *Shock waves in the toda lattice: Analysis*, Phys. Rev. A **24** (1981), no. 5, 2595–2623.
- [HL91] T. Y. Hou and P. Lax, *Dispersive approximations in fluid dynamics*, Comm. Pure Appl. Math. **44** (1991), 1–40.
- [HLM94] M.H. Hays, C. D. Levermore, and P.D. Miller, *Macroscopic lattice dynamics*, Physica D **79** (1994), no. 1, 1–15.
- [HLW02] E. Hairer, Ch. Lubich, and G. Wanner, *Geometric Numerical Integration*, Springer Series in Comp. Mathem., vol. 31, Springer, Berlin, 2002.
- [Hör97] L. Hörmander, *Lectures on Nonlinear Hyperbolic Differential Equations*, Mathématiques & Applications, vol. 26, Springer, Paris, 1997.
- [HR07] M. Herrmann and J. Rademacher, *Dispersive and non-classical shocks in fpu chains*, in preparation, 2007.
- [HS78] B. L. Holian and G. K. Straub, *Molecular dynamics of shock waves in one-dimensional chains*, Phys. Rev. B **18** (1978), 1593–1608.

- [Kam91] S. Kamvissis, *On the long time behavior of the double infinite toda chain under shock initial data*, Ph.D. thesis, New York University, 1991.
- [Lax86] P.D. Lax, *On dispersive difference schemes*, *Physica D* **18** (1986), 250–254.
- [Lax91] ———, *The zero dispersion limit, a deterministic analogue of turbulence*, *Comm. Pure Appl. Math.* **44** (1991), 1047–1056.
- [LeF02] P. G. LeFloch, *Hyperbolic Conservation Laws*, *Lectures in Mathematics: ETH Zürich*, Birkhäuser, Basel, 2002.
- [LL83] P.D. Lax and C.D. Levermore, *The small dispersion limit of the Korteweg-de Vries equation, I, II, III*, *Comm. Pure Appl. Math.* **36** (1983), no.3, 253–290; no.5, 571–593; no.6, 809–830.
- [LL96] C.D. Levermore and J.G. Liu, *Large oscillations arising in a dispersive numerical scheme*, *Physica D* **99** (1996), 191–216.
- [LLV93] P. D. Lax, C. D. Levermore, and S. Venakides, *The generation and propagation of oscillations in dispersive initial value problems and their limiting behavior*, *Important developments in soliton theory* (A.S. Fokas and V.E. Zakharov, eds.), Springer, Berlin, 1993, pp. 205–241.
- [Mac02] F. Maciá, *Propagación y control de vibraciones en medios discretos y continous*, Ph.D. thesis, Universidad Complutense de Madrid, 2002.
- [Mac04] ———, *Wigner measures in the discrete setting: high-frequency analysis of sampling and reconstruction operators*, *SIMA* **36** (2004), no. 2, 347–383.
- [Mie06] A. Mielke, *Macroscopic behavior of microscopic oscillations in harmonic lattices using wigner-husimi measures*, to appear in *Arch. Rat. Mech. Analysis*, 2006.
- [Pan05] A. Pankov, *Travelling Waves and Periodic Oscillations in Fermi-Pasta-Ulam Lattices*, Imperial College Press, 2005.
- [PP00] A. A. Pankov and K. Pflüger, *Traveling waves in lattice dynamical systems*, *Math. Meth. Appl. Sci.* **23** (2000), 1223–1235.
- [Smo94] J. Smoller, *Shock waves and reaction-diffusion equations*, 2. ed., *Grundlehren d. mathem. Wissenschaften*, vol. 258, Springer, 1994.
- [Str64] G. Strang, *Accurate partial difference methods, ii nonlinear problems*, *Num. Math.* (1964), no. 6, 37–46.
- [SW00] G. Schneider and C. E. Wayne, *Counter-propagating waves on fluid surfaces and the continuum limit for the Fermi-Pasta-Ulam model*, *International Conference on Differential Equations* (K. Gröger, B. Fiedler, and J. Sprekels, eds.), World Scientific, 2000, pp. 390–403.
- [SYS97] R. D. Skeel, G. Yang, and T. Schlick, *A family of symplectic integrators: Stability, accuracy, and molecular dynamics Applications*, *SIAM J. Sci. Comput.* **18** (1997), 203–222.

- [Tay96] M. E. Taylor, *Partial Differential Equations III: Nonlinear Theory*, Applied Mathematical Sciences, vol. 117, Springer, New York, 1996.
- [Tod81] M. Toda, *Theory of nonlinear lattices*, Springer Series in Solid-State Sci., vol. 20, Springer, Berlin, 1981.
- [VDO91] S. Venakides, P. Deift, and R. Oba, *The Toda shock problem*, Comm. Pure Appl. Math. **44** (1991), 1171–1242.
- [Ven85] S. Venakides, *The generation of modulated wavetrains in the solution of the Korteweg-de Vries equation*, Comm. Pure Appl. Math. **38** (1985), 883–909.
- [War99] G. Warnecke, *Analytische Methoden in der Theorie der Erhaltungsgleichungen*, Teubner Texte z. Mathem., vol. 138, B.G. Teubner, 1999.
- [Whi74] G. B. Whitham, *Linear and Nonlinear Waves*, Pure And Applied Mathematics, vol. 1237, Wiley Interscience, New York, 1974.